

**A STUDY ON WAVE PREDICTION USING PARAMETRIC
WAVE MODEL
(CASE STUDY OF WAVES IN THE GULF OF THAILAND)**



**A THESIS SUBMITTED IN PARTIAL FULFILLMENT
OF THE REQUIREMENTS FOR
THE DEGREE OF MASTER OF SCIENCE
(APPLIED MATHEMATICS)
FACULTY OF GRADUATE STUDIES
MAHIDOL UNIVERSITY
2003**

**ISBN 974-04-4114-9
COPYRIGHT OF MAHIDOL UNIVERSITY**

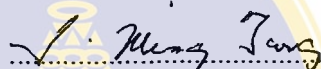
Thesis
Entitled

**A STUDY ON WAVE PREDICTION USING PARAMETRIC
WAVE MODEL
(CASE STUDY OF WAVE IN THE GULF OF THAILAND)**



.....

Mr. Cham Khetchaturat
Candidate



.....

Prof. I. Ming Tang, Ph.D.
Major-Advisor



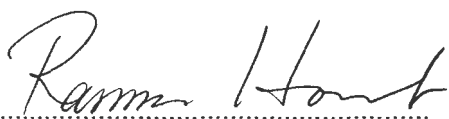
.....

Asst. Prof. Seree Sutharatid, Ph.D.
Co-Advisor



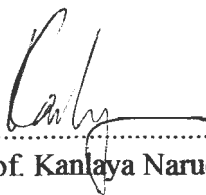
.....

Assoc. Prof. Benchawan Wiwatanapataphee,
Ph.D.
Co-Advisor



.....

Assoc. Prof. Rassmidara Hoonsawat,
Ph.D.
Dean
Faculty of Graduate Studies



.....

Asst. Prof. Kanlaya Naruedomkul, Ph.D.
Chair
Master of Science Programme
in Applied Mathematics
Faculty of Science

Thesis
Entitled

**A STUDY ON WAVE PREDICTION USING PARAMETRIC
WAVE MODEL
(CASE STUDY OF WAVE IN THE GULF OF THAILAND)**

was submitted to the Faculty of Graduate Studies, Mahidol University
for the degree of Master of Science(Applied Mathematics)

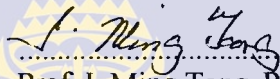
on

October 6, 2003



.....

Mr. Charn Khetchaturat
Candidate



.....

Prof. I. Ming Tang, Ph.D.
Chair



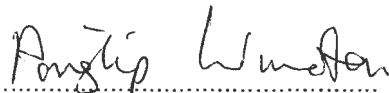
.....

Asst. Prof. Seree Sutharatid, Ph.D.
Member



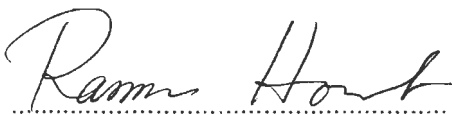
.....

Assoc. Prof. Benchawan Wiwatanapataphee,
Ph.D.
Member



.....

Assoc. Prof. Pongtip Winotai, Ph.D.
Member



.....

Assoc. Prof. Rassmidara Hoonsawat,
Ph.D.
Dean
Faculty of Graduate Studies
Mahidol University



.....

Prof. Amaret Bhumiratana,
Ph.D.
Dean
Faculty of Science
Mahidol University

ACKNOWLEDGEMENT

I would like to express my sincere gratitude and deep appreciation to my major advisor, Prof. Dr. I. Ming Tang, for his kindness, advice guidance, and encouragement throughout this research which enabled me to carry out this thesis successfully. All his kindness, generosity and sympathy will be long remembered with respect.

I am also grateful to Asst. Prof. Seree Sutharatid and Assoc.Prof. Benchawan Wiwatanapataphee my co-advisors for their kindness, helpful comments, guidance and advice concerning this thesis.

I am deeply indebted to my external committee, Assoc. Prof. Pongtip Winotai for his valuable advice and comments and his kindness and understanding throughout the study.

My special appreciation is expressed Mr. Wattana Kanbua, for access to the data, excellent comments and creative guidance throughout the work of my thesis.

I am also particularly grateful to all members of Mathematics Department for their help, friendship and encouragement.

Charn Khetchaturat

**A STUDY ON WAVE PREDICTION USING PARAMETRIC WAVE MODEL
(CASE STUDY OF WAVES IN THE GULF OF THAILAND).**

CHARN KHETCHATURAT 4137882 SCAM/M

M.Sc.(APPLIED MATHEMATICS)

**THESIS ADVISORS : I. MING TANG, Ph.D., SEREE SUTHARATID, Ph.D.,
BENCHAWAN WIWATANAPATAPHEE, Ph.D.**

ABSTRACT

Wave prediction was study by using parametric wave models. The basic parametric wave model was developed by using least square fitting for prediction of the wave characteristics in the Gulf of Thailand. We also adjusted the parameter of the studied model and in addition the artificial neural network (ANN) was applied to forecast waves. Comparing all of the parametric wave models in this research, the results indicated that the developed model was the best method of prediction of significant wave periods. The adjusted parameter model predicted better than the previous unadjusted model. However, the prediction by the artificial neural network was best in both significant wave periods and significant wave heights.

**KEY WORDS : WAVE PREDICTION/ PARAMETRIC MODEL / LEAST
SQUARE FITTING / GULF OF THAILAND / ARTIFICIAL
NEURAL NETWORK / SIGNIFICANT WAVE PERIOD /
SIGNIFICANT WAVE HEIGHT**

74 P. ISBN 974-04-4114-9

การศึกษาการพยากรณ์คลื่น โดยแบบจำลองเชิงสถิติ(กรณีศึกษาคลื่นในอ่าวไทย)
(A STUDY ON WAVE PREDICTION USING PARAMETRIC WAVE MODEL
(CASE STUDY OF WAVES IN THE GULF OF THAILAND)).

ชาญ เขตจัตุรัส 4137882 SCAM/M

วท.ม. (คณิตศาสตร์ประยุกต์)

คณะกรรมการควบคุมวิทยานิพนธ์ : ไอ. มิ่ง ถัง, Ph.D., เสรี สุทธาราทีศย์, Ph.D., เบญจวรรณ วิ-
วัฒน์ปฐพี, Ph.D.

บทคัดย่อ

การพยากรณ์คลื่นโดยใช้แบบจำลองเชิงสถิติได้ถูกศึกษา แบบจำลองเชิงสถิติอย่างง่ายได้
ถูกพัฒนาขึ้น โดยใช้วิธีกำลังสองน้อยสุด เพื่อพยากรณ์คลื่นในอ่าวไทย เราได้ปรับแต่งพารามิเตอร์
ของ แบบจำลองเชิงสถิติที่ได้ศึกษาด้วย และนอกจากนี้ยังได้ใช้ โครงข่ายประสาทเทียม เพื่อ
พยากรณ์คลื่น ผลจากการเปรียบเทียบ แบบจำลองเชิงสถิติทุกแบบจำลองที่ได้ศึกษางานวิจัยนี้ พบว่า
แบบจำลองที่ถูกพัฒนาขึ้น พยากรณ์ คาบคลื่นอย่างมีนัยสำคัญได้ดีที่สุด แบบจำลองที่ถูกปรับแต่ง
พารามิเตอร์พยากรณ์ได้ดีขึ้นกว่าเดิม อย่างไรก็ตามการพยากรณ์คลื่นโดยใช้โครงข่ายประสาทเทียม
ให้ผลการพยากรณ์ ทั้งคาบคลื่นอย่างมีนัยสำคัญ และ ความสูงคลื่นอย่างมีนัยสำคัญได้ดีที่สุด

74 หน้า. ISBN 974-04-4114-9

CONTENTS

	Page
ACKNOWLEDGEMENT	iii
ABSTRACT	iv
LIST OF TABLES	viii
LIST OF FIGURES	x
LIST OF NOTATION AND SYMBOL	xiv
CHAPTER	
I INTRODUCTION	1
General	1
Literature Review	1
Objectives of the Study	3
Expected Benefits	3
II BACKGROUND OF STUDY	4
Introduction	4
The Basic Tenet Wave Growth Model	4
Others Wave Growth Models	5
Thompson Model	5
SMB Model	7
TMA Model	9
The Neural Network Model	10
Neuron Model	10
Single Layer of Neurons	10
Multilayer Neural Network	11
Neural Network with Wave Parametric Inputs	12
III METHODOLOGY	14
Polynomials Least-Square Fitting	14
Multiple Linear Least-Square Fitting	16

CONTENTS(Continued)

vii
Page

Nonlinear Least-Square Fitting	17
General Method	17
Linearization of Nonlinear Least-square fitting	18
Backpropagation Algorithm	19
Performance Measurement	21
IV EXPERIMENTS AND RESULTS	22
Data	22
Experiments	24
Results	46
V CONCLUSION	54
REFERENCES	56
APPENDIX	58
Program Listing For Least Square Fitting	59
BIOGRAPHY	74

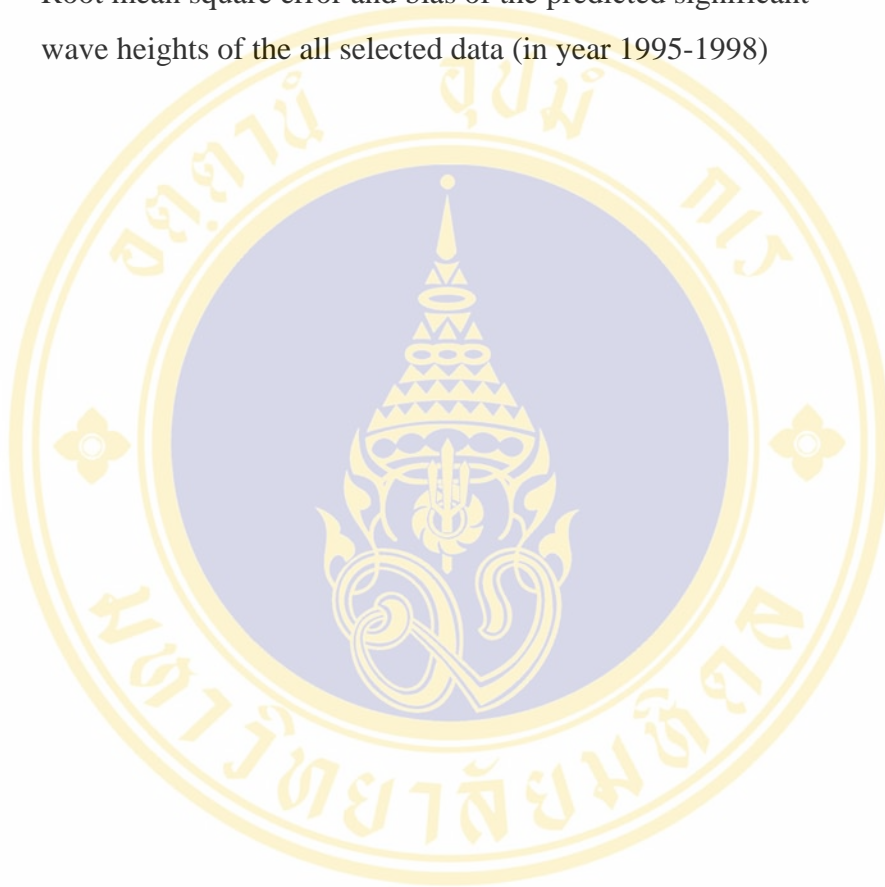
LIST OF TABLES

Table		Page
2.1	Derived coefficients of the Thompson model.	7
2.2	Derived exponents of the Thompson model.	7
2.3	Derived constants of the drag coefficient C_D of the Thompson model.	7
2.4	Derived coefficients of the SMB model.	8
2.5	Derived coefficients of the SMB model.	8
2.6	Derived exponents of the SMB model.	8
2.7	Derived coefficients of the TMA model.	9
2.8	Derived exponents of the TMA model.	9
4.1	Mean of concerned parameters of the data in 17 March 1998 to 8 April 1998	32
4.2	Root mean square error (RMSE) and bias (BIAS) of least-square fitting of wind speed and significant wave height of the data in 17 March 1998 to 8 April 1998	35
4.3	Root mean square error (RMSE) and bias (BIAS) of least-square fitting of wind speed and significant wave period of the data in 17 March 1998 to 8 April 1998	38
4.4	Range of the fetch length of the data in 25 August 1995 to 25 September 1995	39
4.5	Root mean square error (RMSE) and bias (BIAS) of least-square fitting of the fetch length and dimensionless significant wave height of the data in 25 August 1995 to 25 September 1995	42
4.6	Root mean square error and bias of least-square fitting of fetch length And dimensionless significant wave period of the data period in 25 August 1995 to 25 September 1995	45

LIST OF TABLES (Continued)

ix

Table		Page
4.7	Root mean square error and bias of the predicted significant wave periods of the all selected data (in year 1995-1998)	53
4.7	Root mean square error and bias of the predicted significant wave heights of the all selected data (in year 1995-1998)	53



LIST OF FIGURES

Figure	Page
2.1 An Artificial Neuron	10
2.2 Two-layer neural network	11
2.3 Network structure for significant wave height prediction	12
2.4 Network structure for significant wave period prediction	13
4.1.1 Representation of topography area of and location of UNOCAL buoy station.	23
4.2.1 Wave parameters plots in time.	24
4.2.2 Scatter plots of speed and direction of wind in 15 January 1995 to 3 March 1995.	25
4.2.3 Scatter plots of speed and direction of wind in 25 August 1995 to 25 September 1995.	26
4.2.4 Scatter plots of speed and direction of wind in 22 August 1996 to 20 September 1996.	27
4.2.5 Scatter plots of speed and direction of wind 8 December 1996 to 31 December 1996.	28
4.2.6 Scatter plots of speed and direction of wind in 18 August 1997 to 25 August 1997	29
4.2.7 Scatter plots of speed and direction of wind in 2 December 1997 to 28 December 1997.	30
4.2.8 Scatter plots of speed and direction of wind, in 17 March 1998 to 8 April 1998	31
4.2.9 Scatter plots and curves of nonlinear least-square fits of wind speed and significant wave height in 17 March 1998 to 8 April 1998	32
4.2.10 Scatter plots and curves of least-square fits parabola of wind speed and significant wave height in 17 March 1998 to 8 April 1998	33
4.2.11 Scatter plots and curves of least-square cube of wind speed	

LIST OF FIGURES (Continued)

xi

Figure	Page
and significant wave height in 17 March 1998 to 8 April 1998	33
4.2.12 Scatter plots and curves of least-square polynomial degree 4 of wind speed and significant wave height in 17 March 1998 to 8 April 1998	34
4.2.13 Scatter plots and curve of least-square polynomial degree 5 of wind speed and significant wave height in 17 March 1998 to 8 April 1998	34
4.2.14 Scatter plots and curve of nonlinear least-square fits of wind speed and significant wave period in 17 March 1998 to 8 April 1998	35
4.2.15 Scatter plots and curve of least-square parabola of wind speed and significant wave period in 17 March 1998 to 8 April 1998	36
4.2.16 Scatter plots and curve of least-square cube of wind speed and significant wave period in 17 March 1998 to 8 April 1998	36
4.2.17 Scatter plots and curve of least-square polynomial degree 4 of wind speed and significant wave period in 17 March 1998 to 8 April 1998	37
4.2.18 Scatter plots and curve of least-square polynomial degree 5 of wind speed and significant wave period in 17 March 1998 to 8 April 1998	37
4.2.19 Scatter plots and curve of nonlinear least-square fits of fetch length and dimensionless significant wave height in 25 August 1995 to 25 September 1995	39
4.2.20 Scatter plots and curve of least-square parabola fits of fetch length and dimensionless significant wave height in 25 August 1995 to	

LIST OF FIGURES (Continued)

xii

Figure	Page
25 September 1995	40
4.2.21 Scatter plots and curve of least-square parabola fits of fetch length and dimensionless significant wave height in 25 August 1995 to 25 September 1995	40
4.2.22 Scatter plots and curve of least-square polynomial degree 4 fits of fetch length and dimensionless significant wave height in 25 August 1995 to 25 September 1995	41
4.2.23 Scatter plots and curve of least-square polynomial degree 5 fits of fetch length and dimensionless significant wave height in 25 August 1995 to 25 September 1995	41
4.2.24 Scatter plots and curve of nonlinear least-square fits of fetch length And dimensionless significant wave period in 25 August 1995 to 25 September 1995	42
4.2.25 Scatter plots and curve of least-square parabola fits of fetch length and dimensionless significant wave period in 25 August 1995 to 25 September 1995	43
4.2.26 Scatter plots and curve of least-square cube fits of fetch length and dimensionless significant wave period in 25 August 1995 to 25 September 1995	43
4.2.27 Scatter plots and curve of least-square polynomial degree 4 fits of fetch length and dimensionless significant wave period in 25 August 1995 to 25 September 1995	44
4.2.28 Scatter plots and curve of least-square polynomial degree 5 fits of fetch length and dimensionless significant wave period in 25 August 1995 to 25 September	44
4.2.29 Shows the begin of data for fitting wave growth with duration	46

LIST OF FIGURES (Continued)

xiii

Figure	Page
4.3.1 Scatter plots of the significant wave periods predicted by the SMB model of the all selected data	47
4.3.2 Scatter plots of the significant wave heights predicted by the SMB model of the all selected data	47
4.3.3 Scatter plots of the significant wave heights predicted by the SMB model of the all selected data	48
4.3.4 Scatter plots of the significant wave heights predicted by the Thompson model of the all selected data	48
4.3.5 Scatter plots of the significant wave periods predicted by the TMA model of the all selected data	49
4.3.6 Scatter plots of the significant wave heights predicted by the TMA model of the all selected data	49
4.3.7 Scatter plots of the significant wave periods predicted by the developed parametric model of the all selected data	50
4.3.8 Scatter plots of the significant wave heights predicted by the developed parametric model of the all selected data	50
4.3.9 Scatter plots of the significant wave periods predicted by the adjusted parameter of the TMA of the all selected data	51
4.3.10 Scatter plots of the significant wave heights predicted by the adjusted parameter of the TMA of the all selected data	51
4.3.11 Scatter plots of the significant wave periods predicted by the trained parametric inputs neural network of the all selected data	52
4.3.12 Scatter plots of the significant wave heights predicted by the trained parametric inputs neural network of the all selected data	52

LIST OF NOTATION AND SYMBOL

SYMBOL	MEANING	PAGE FIRST USED
1. \tilde{F}	Dimensionless of F	4
2. F	Fetch length	4
3. t	Time duration	4
4. H_s	Significant wave height	4
5. T_s	Significant wave period	4
6. H_∞	Fully developed significant wave height	5
7. T_∞	Fully developed significant wave period	6
8. C_D	The drag coefficient	6
9. u_{10}	Wind speed at 10 meters elevation	6
10. $p_m(x)$	Polynomial of degree m	14
11. E	Sum of squared error	14
12. $\theta^{(r)}$	The value of θ in the r^{th} step	17
13. $Q_{ji}^{(r)}$	Stand for $\left. \frac{\partial}{\partial \theta_j} f(x_i, \theta) \right _{\theta=\theta^{(r)}}$	17
14. $sQQ_{st}^{(r)}$	Stand for $\sum_{i=1}^n Q_{si}^{(r)} Q_{ti}^{(r)}$	18
15. $seQ_j^{(r)}$	Stand for $\sum_{i=1}^n [y_i - f(x_i, \theta^{(r)})] Q_{ji}^{(r)}$	18
16. η	Learning rate of backpropagation algorithm	20
17. α	Momentum of backpropagation algorithm	20
18. INP_{ip}	The input value of the i^{th} neuron and the p^{th} pattern	20
19. $RMSE$	The relative root mean square error	21
20. $BIAS$	The bias of predicted data	21

CHAPTER I

INTRODUCTION

1.1 General

The Gulf of Thailand is under the influence of monsoon winds of seasonal character i.e. southwest monsoon and northeast monsoon. Southwest monsoon usually starts in mid-May and ends in mid-October while northeast monsoon normally starts in mid-October and ends in mid-February. Waves influenced the monsoon in the Gulf of Thailand affect the Thai fishermen and many other marine activities e.g. oil and gas exploration.

1.2 Literature Review

The study of wave generation has had a long and rich history. Beginning with the classic works of Kelvin (1887) and Helmholtz (1888) in the 1800's, many scientists, engineers, and mathematicians have addressed various forms of water wave motions and their interactions with the wind. In the early 1900's, Jeffreys (1924, 1925) hypothesized that waves created a "sheltering effect" and hence create a positive feedback mechanism for transfer of momentum into the wave field from the wind. However, it was not until World War II that organized wave predictions began in earnest. During the 1940's, large bodies of wave observations were collected and the base for empirical wave predictions was made possible. Sverdrup and Munk (1947) presented the first proposed relationships among various wave-generation parameters and resulting wave conditions. Bretschneider (1952) revised these relationships based on additional evidence. The methods derived from these exemplary pioneer works are still in active use today.

In the 1950's, researchers began to recognize that the wave generation process was best described as a spectral phenomenon (e.g. Pierson, Neumann, and James (1955)). Phillips (1958) and Miles (1957) advanced two theories that formed the cornerstone of the understanding of wave generation physics for many years. Phillips'

contribution involved the resonant interactions of turbulent pressure fluctuations with waves propagating at the same speed. Miles' contribution centered on the mean flux of momentum from a "matched layer" above the wave field into waves traveling at the same speed. Phillips' theory predicted linear wave growth and was believed to control the early stages of the wave growth. Miles' theory predicted an exponential growth and was believed to control the major portion of wave growth observed in nature. Direct measurements of the Phillips' resonance mechanism indicated that the measured turbulent fluctuations were too small by about an order of magnitude to explain the observed early growth in waves. It is still however accepted as a plausible concept. Subsequent work by Snyder and Cox (1966) and Snyder et al. (1981) have supported at least the functional form of Miles' theory for the transfer of energy into the wave field from the winds.

From the basic concepts of energy conservation and the fact that waves do attain limiting fully developed wave heights, it is obvious that wave generation physics cannot consist of only wind source terms. There must be some physical mechanism or mechanisms that leads to a balance of wave growth and dissipation for the case of fully developed conditions. Phillips (1958) postulated that one such mechanism in waves would be wave breaking. Based on dimensional considerations and the knowledge that wave breaking has a very strong local effect on waves, Phillips argued that energy densities within a spectrum would always have a universal limiting value.

Kitaigorodskii (1962) extended the arguments of Phillips to distinct regions throughout the entire spectrum where different mechanisms may be important. Pierson and Moskowitz (1964) followed the dimensional arguments of Phillips and supplemented these arguments, with relationships derived from measurements at sea. They extended the form of Phillips spectrum to the classical Pierson-Moskowitz spectrum.

It was noted (first by Phillips, 1958) that at higher frequencies than the peak frequency, the energy in a given wave-field 'saturates'. This saturation produces relatively equivalent energies for a given frequency regardless of virtually all other parameters. Considerable data taken off the western shore of Denmark was used to produce a model of the wave spectrum (Hasselmann, 1973).

Donelan et al. (1985) proposed a popular alternative which combines the relatively weak effects due to fetch into a single formulation. The formulation also accounts for directionality of the wind. Donelan, like SMB and conventional JONSWAP, does not account for water depth. However, these models are extremely popular and are often used in shallow-water situations. For a good review of the pluses and minuses of these deep-water models.

To correct for depth-dependent effects, Bouws et al. (1985) also manipulated the linear term. They wanted it to reflect the loss of energy due to enhance dissipation in shallow water.

1.3 Objectives of the Study

The purpose of this study is to apply the parametric model for prediction of the wave in the Gulf of Thailand.

1.4 Expected Benefits

This study is expected to be helpful in the other or wave climate research and give rise to better understanding waves influenced monsoon in the Gulf of Thailand.

CHAPTER II

BACKGROUND OF STUDY

2.1 Introduction

Parametric wave model is a wave model based on large numbers of wave measurements for various wind speeds, wind durations and fetch lengths. Wind duration means the time in which the wind lasts. Fetch length means distance across which wind interacts with the water surface. From these measurements wave growth lines are identified. In the other word, simple parametric wave model is a statistical best-fit model tuned to many wave observations.

There are many empirical formulae for wave growth. These formulae are deduced by analyzing a great number of visual observations by graphical method using known parameters of wave characteristics.

2.2 The Basic Tenet Wave Growth Model

In representing wave growth formulae, the variables are all made dimensionless through the definitions (WHO, 1995).

$$\tilde{F} = \frac{gF}{U^2} \quad (2.2.1)$$

$$\tilde{t} = \frac{gt}{U} \quad (2.2.2)$$

$$\tilde{d} = \frac{gd}{U^2} \quad (2.2.3)$$

$$\tilde{H}_s = \frac{gH}{U^2} \quad (2.2.4)$$

$$\tilde{T}_s = \frac{gT}{U} \quad (2.2.5)$$

where F , t , d , H_s , T_s , U and g are fetch length, wind duration, water depth, wave height, wave period, wind speed and acceleration of gravity respectively.

Oceanographers expect that waves will reach a stationary fetch-limited state of development for a constant wind speed and direction over a fixed fetch. In this situation, wave heights will remain constant through time but will vary along the fetch (Patrick, 2001). Then fetch-limited wave heights is expected to be given by

$$\tilde{H}_s = \lambda_1 \tilde{F}^{m_1}, \quad (2.2.6)$$

where λ_1 is dimensionless coefficient and

m_1 is dimensionless exponent.

From basic conservation laws and the dispersion relationship, it is anticipated that any law governing the rate of growth of waves along a fetch will also form a unique constraint on the rate of growth of waves through time. Then duration-growth of waves will be given by

$$\tilde{H}_s = \lambda_2 \tilde{t}^{m_2}, \quad (2.2.7)$$

where λ_2 is dimensionless coefficient and

m_2 is dimensionless exponent.

Duration limited by fetch length is now expressed as:

$$\tilde{t} = \lambda_3 \tilde{F}^{m_3}, \quad (2.2.8)$$

where λ_3 is dimensionless coefficient and

m_3 is dimensionless exponent.

Fully developed wave height could be given as

$$\tilde{H}_\infty = \lambda_4, \quad (2.2.9)$$

where \tilde{H}_∞ is fully developed wave height and

λ_4 is dimensionless coefficient .

We call this model that the basic parametric model.

2.3 The Others Wave Growth Models

2.3.1 Thompson Model

This model is developed by Thompson (1996) and formulated base on the basic parametric model. Duration with fetch-limited can be written as

$$\tilde{t} = \lambda_5 F^{m_5}, \quad (2.3.1.1)$$

where λ_5 is dimensionless coefficient and

m_5 is dimensionless exponent.

Wave growth with fetch is

$$\tilde{H}_s = \lambda_6 \tilde{F}^{m_6}, \quad (2.3.1.2)$$

where λ_6 is dimensionless coefficient and

m_6 is dimensionless exponent.

Wave period with fetch is

$$\tilde{T}_s = \lambda_7 \tilde{F}^{m_7}, \quad (2.3.1.3)$$

where λ_7 is dimensionless coefficient and

m_7 is dimensionless exponent.

Fully developed wave conditions in these equations are given by

$$\tilde{H}_\infty = \lambda_8 \quad (2.3.1.4)$$

and

$$\tilde{T}_\infty = \lambda_9, \quad (2.3.1.5)$$

where λ_8 and λ_9 are dimensionless coefficients.

Fetch in term of duration-limited is given by

$$\tilde{F} = \lambda_{10} \tilde{t}^{m_{10}}, \quad (2.3.1.6)$$

where λ_{10} is dimensionless coefficient and

m_{10} is dimensionless exponent.

The velocity of wind in the equations 2.3.1.1 to 2.3.1.6 is given by

$$U = \sqrt{C_D} u_{10} \tag{2.3.1.7}$$

and

$$C_D = c_1 + c_2 u_{10} \tag{2.3.1.8}$$

where C_D is the drag coefficient, u_{10} is wind speed at 10 meters elevation c_1 and c_2 are constants.

The coefficients, exponents and constants of the relations have been derived from large data sets which shown in the table 2.1 to 2.3 (Patrick, 2001).

Table 2.1 Derived coefficients of the Thompson model.

Dimensionless coefficients	λ_5	λ_6	λ_7	λ_8	λ_9	λ_{10}
Values	7.8726	0.0413	0.3667	211.5	239.8	0.00523

Table 2.2 Derived exponents of the Thompson model.

Dimensionless exponents	m_5	m_6	m_7	m_8	m_9	m_{10}
Values	7.8726	0.0413	0.3667	211.5	239.8	0.00523

Table 2.3 Derived constants of the drag coefficient C_D of the Thompson model.

Constants	c_1	c_2
Values	0.0011	0.000035

2.3.2 SMB Model

This model was developed by Sverdrup, Munk and Brestschneider (1952). In the SMB model duration with fetch-limited is given by

$$\tilde{t} = \lambda_{11} \exp \left\{ \sqrt{\lambda_{12} \left(\left[\ln(\tilde{F}) \right]^2 - \lambda_{13} \ln(\tilde{F}) + \lambda_{14} \right) + \lambda_{15} \ln(\tilde{F})^2} \right\}, \tag{2.3.2.1}$$

where λ_{11} , λ_{12} , λ_{13} , λ_{14} and λ_{15} are dimensionless coefficients.

Wave growth with fetch is given by

$$\tilde{H}_s = \lambda_{16} \tanh \left[\lambda_{17} (\tilde{F})^{m_{11}} \right], \quad (2.3.2.2)$$

where λ_{16} and λ_{17} are dimensionless coefficients and m_{11} is dimensionless exponent.

Wave period with fetch is given by

$$\tilde{T}_s = \lambda_{19} \pi \tanh \left[\lambda_{20} (\tilde{F})^{m_{12}} \right] \quad (2.3.2.3).$$

where λ_{19} and λ_{20} are dimensionless coefficients and m_{12} is dimensionless exponent.

The coefficients and exponents of the relations have been derived from large data sets, using a statistical best-fit, shown in the table 2.4 to 2.6. (Bretschneider, 1952).

Table 2.4 Derived coefficients of the SMB model.

Dimensionless coefficients	λ_{11}	λ_{12}	λ_{13}	λ_{14}	λ_{15}
Values	6.5882	0.0161	0.3692	2.2024	0.8798

Table 2.5 Derived coefficients of the SMB model.

Dimensionless coefficients	λ_{16}	λ_{17}	λ_{18}	λ_{19}	λ_{20}
Values	0.283	0.0125	0.3692	2.4	0.077

Table 2.6 Derived exponents of the SMB model.

Dimensionless exponents	m_{11}	m_{12}
Values	0.42	0.25

2.3.3 TMA Model

The Thompson and SMB model did not consider the depth of the sea, the formulation for depth-dependent effects. The TMA Model (Bouws et al. 1985) does this, ie., it includes depth-dependent effects. The model gives

$$\tilde{H}_s = \lambda_{21} \tanh(\lambda_{22} \tilde{d}^{m_{13}}) \tanh \left[\frac{\lambda_{23} \tilde{F}^{m_{14}}}{\tanh(\lambda_{22} \tilde{d}^{m_{13}})} \right] \tag{2.3.3.1}$$

and

$$\tilde{T}_s = 2\pi\lambda_{24} \tanh(\lambda_{25} \tilde{d}^{m_{15}}) \tanh \left[\frac{\lambda_{26} \tilde{F}^{m_{16}}}{\tanh(\lambda_{25} \tilde{d}^{m_{15}})} \right], \tag{2.3.3.2}$$

where $\lambda_{21}, \lambda_{22}, \lambda_{23}, \lambda_{24}, \lambda_{25}$ and λ_{26} are dimensionless coefficients and m_{13}, m_{14}, m_{15} and m_{16} are dimensionless exponents.

The values of the coefficients have been estimated by many investigators. According to CERC (Coastal Engineering Research Center) the coefficients have been shown in the table 2.7 and 2.8 (WMO, 1995).

Table 2.7 Derived coefficients of the TMA model.

Dimensionless coefficients	λ_{21}	λ_{22}	λ_{23}	λ_{24}	λ_{25}	λ_{26}
Values	0.283	0.520	0.0125	1.2	0.833	0.077

Table 2.8 Derived exponents of the TMA model.

Dimensionless exponents	m_{13}	m_{14}	m_{15}	m_{16}
Values	0.75	0.42	0.375	0.25

2.4 The Neural Network Model

2.4.1 Artificial Neuron Model

The most commonly used neuron model, based on the model proposed by McCulloch and Pitts in 1943 (Page, Gomm and Williams, 1993) consisted of inputs, a

bias, weights, an activation function and an output. Each neuron input, x_1, x_2, \dots, x_n , is weighted by the values w_1, w_2, \dots, w_n respectively. A bias is assigned by a constant input of 1 weighted by the value w_0 . The output, y , is obtained by summing the weighted inputs to the neuron and passing the result through an activation function, f , as shown in Figure 2.1.

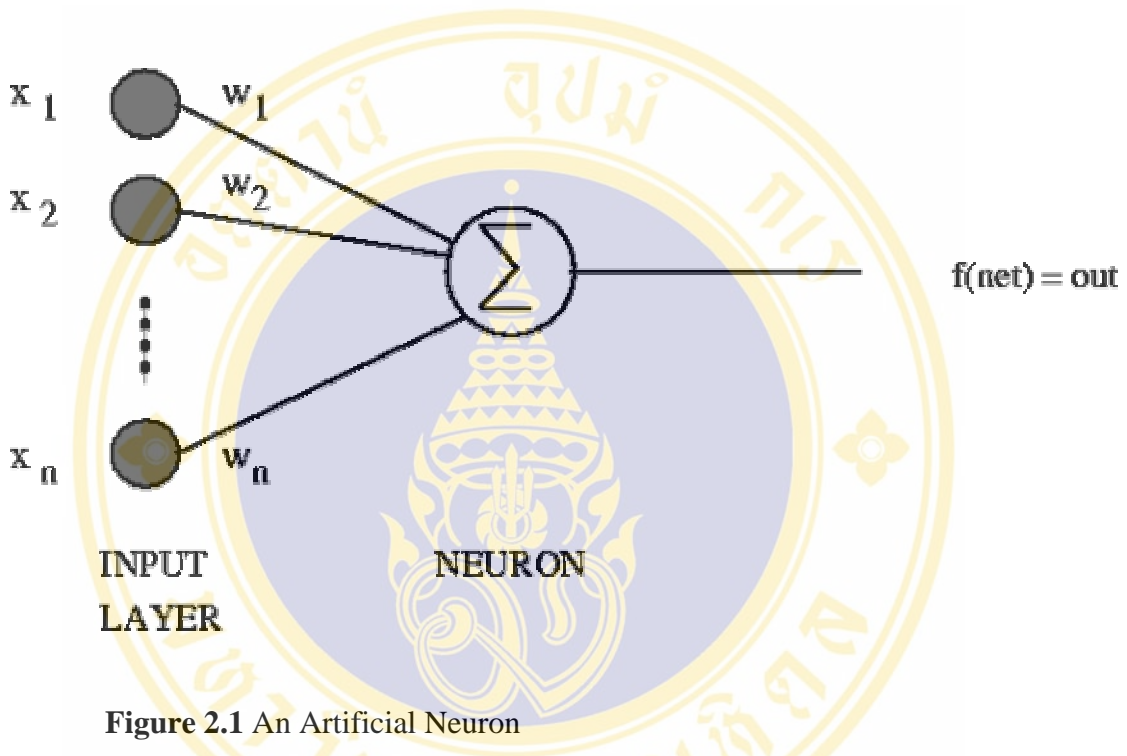


Figure 2.1 An Artificial Neuron

Various types of activation functions are possible such as linear, threshold, sigmoidal and hyperbolic tangent functions.

2.4.2 Single Layer of Neuron

A single layer of neurons consists of I inputs and H neurons, each of all inputs is weighted to each of all neurons.

2.4.3 Multilayer Neural Network

A multilayer neural network consists of several single layer of neurons. The inputs of the network are the inputs of the first layer of neurons and the outputs of the network are the outputs of the last layer of neurons. The layer of neurons is called that

the output layer and the other layers are called the hidden layers. A two-layer neural network is shown in Figure 2.2.

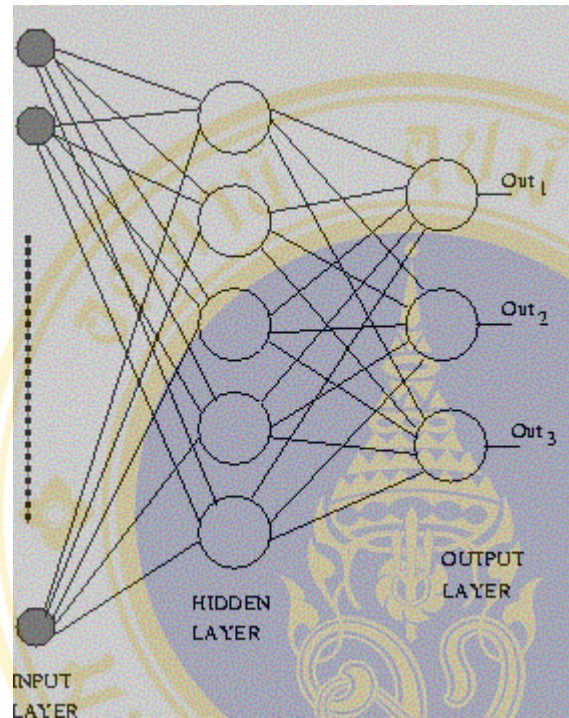


Figure 2.2 Two-layer neural network

The basic idea of training (Schmidt, 1996) is to present the input to the network; calculate in the forward direction the output of each layers and the final output of the network. For the output layer the desired values are known and therefore the weights can be adjusted as for each layer of neurons. One of the most popular training algorithms for multilayer neural network is backpropagation algorithm.

2.4.4 Neural Network with Wave Parametric Inputs

The neural network used in this research, for prediction of significant wave heights, is two-layer neural network as shown in Figure 2.3. The inputs to the network are wind speed, fetch length, wind direction and significant wave height at the $(t-1)^{\text{th}}$ step. The hidden layer consists of 12 neurons. The output layer has one neuron which

refers to the significant wave height at the t^{th} step. The activation function for each hidden neurons and output neuron are the hyperbolic tangent function and the linear function, respectively.

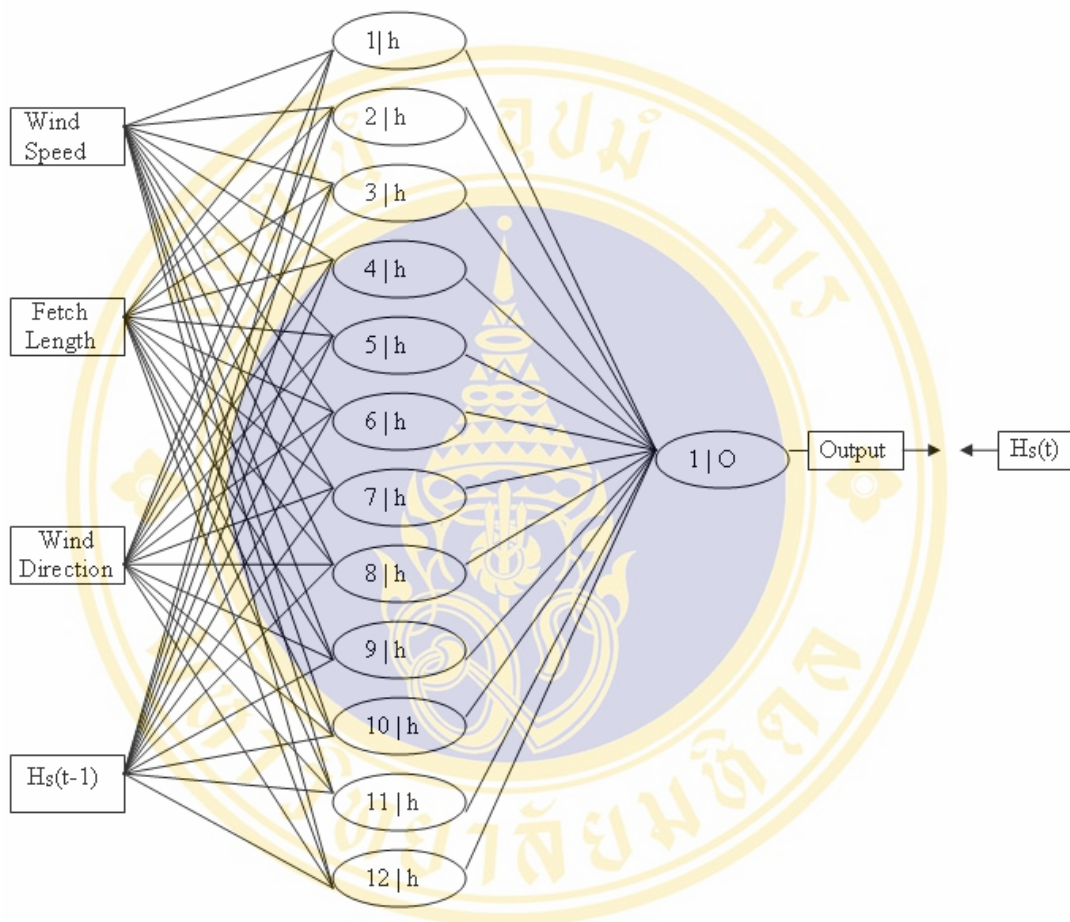


Figure 2.3 Network structure for significant wave height prediction

The neural network, for prediction of significant wave periods has the same structure, as shown in Figure 2.4. The inputs of the network are wind speed, fetch length, wind direction and significant wave period at the $(t-1)^{\text{th}}$ step. The output is the significant wave period at the t^{th} step.

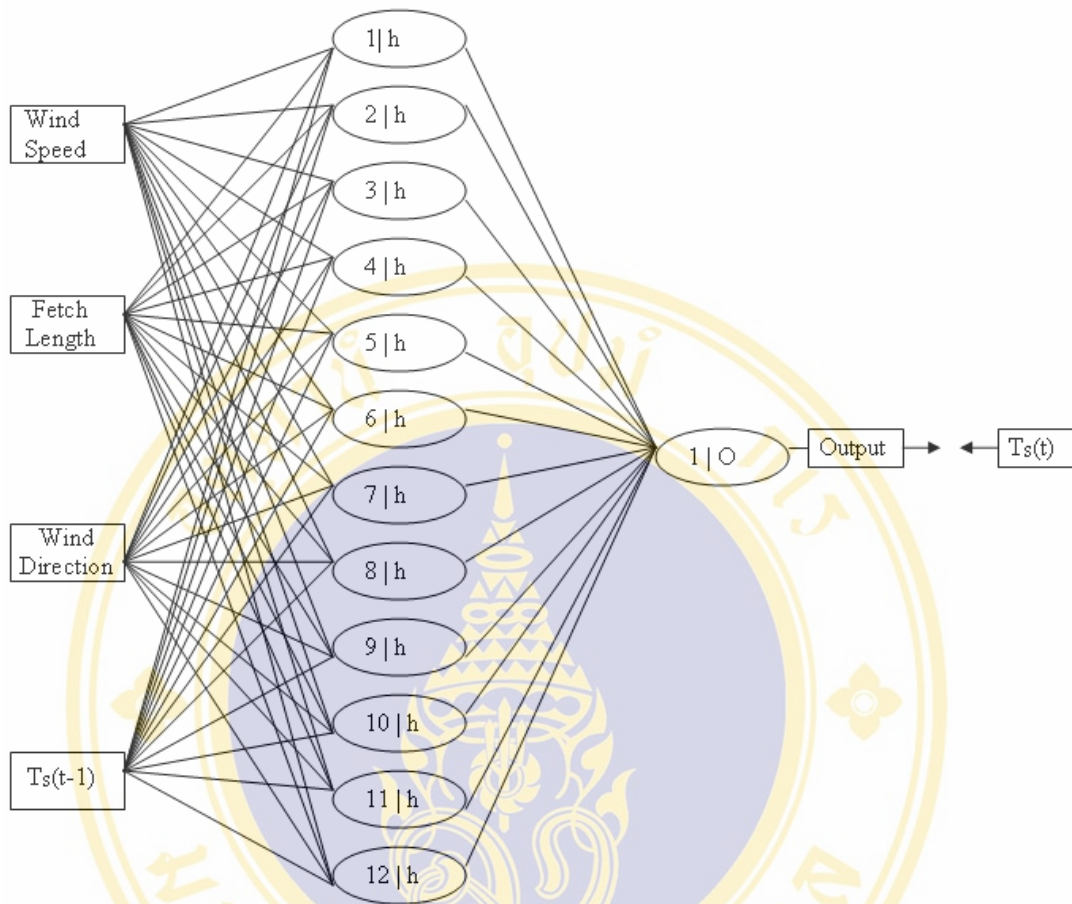


Figure 2.4 Network structure for significant wave period prediction

CHAPTER III

METHODOLOGY

Field data are often accompanied by noise. Even though all control parameters (independent variables) remain constant, the resultant outcomes (dependent variables) vary. A process of quantitatively estimating the trend of the outcomes, also known as regression or curve fitting, therefore becomes necessary.

The curve fitting process fits equations of approximating curves to the raw field data. Nevertheless, for a given set of data, the fitting curves of a given type are generally not unique. Thus, a curve with a minimal deviation from all data points is desired. The best-fitting curve can be obtained by the method of least squares.

3.1 Polynomials Least-Squares Fitting

The least-squares m^{th} degree polynomials method uses m^{th} degree polynomials

$p_m(x) = \sum_{k=0}^m a_k x^k$ to approximate the given set of data, (x_1, y_1) , $(x_2, y_2), \dots, (x_n, y_n)$, where $m \leq n - 1$. This requires choosing the coefficients a_0, a_1, \dots, a_m to minimize the sum of squared errors defined as

$$E = \sum_{i=1}^n (y_i - p_m(x_i))^2. \quad (3.1.1)$$

To obtain the least square error, the unknown coefficients a_0, a_1, \dots, a_m must yield zero first derivatives.

$$\left. \begin{aligned} \frac{\partial E}{\partial a_0} &= 2 \sum_{i=1}^n (y_i - p_m(x_i)) = 0 \\ \frac{\partial E}{\partial a_1} &= 2 \sum_{i=1}^n x_i (y_i - p_m(x_i)) = 0 \\ \frac{\partial E}{\partial a_m} &= 2 \sum_{i=1}^n x_i^m (y_i - p_m(x_i)) = 0 \end{aligned} \right\} \quad (3.1.2)$$

Expanding the above equations, we have

$$\begin{bmatrix} \sum_{i=1}^n x_i^0 & \sum_{i=1}^n x_i^1 & \sum_{i=1}^n x_i^2 & \dots & \sum_{i=1}^n x_i^m \\ \sum_{i=1}^n x_i^1 & \sum_{i=1}^n x_i^2 & \sum_{i=1}^n x_i^3 & \dots & \sum_{i=1}^n x_i^{m+1} \\ \sum_{i=1}^n x_i^m & \sum_{i=1}^n x_i^{m+1} & \sum_{i=1}^n x_i^{m+2} & \dots & \sum_{i=1}^n x_i^{2m} \end{bmatrix} \begin{bmatrix} a_0 \\ a_1 \\ a_m \end{bmatrix} = \begin{bmatrix} \sum_{i=1}^n y_i x_i^0 \\ \sum_{i=1}^n y_i x_i^1 \\ \sum_{i=1}^n y_i x_i^m \end{bmatrix} \quad (3.1.3)$$

For polynomial degree $m = 1$, from the above system of equations, we get the system of the least-squares line as

$$\begin{bmatrix} n & \sum_{i=1}^n x_i \\ \sum_{i=1}^n x_i & \sum_{i=1}^n x_i^2 \end{bmatrix} \begin{bmatrix} a_0 \\ a_1 \end{bmatrix} = \begin{bmatrix} \sum_{i=1}^n y_i \\ \sum_{i=1}^n y_i x_i \end{bmatrix} \quad (3.1.4)$$

For polynomial degree $m = 2$, from the system of equations (3.1.3), we get the system of the least-squares parabola as

$$\begin{bmatrix} n & \sum_{i=1}^n x_i & \sum_{i=1}^n x_i^2 \\ \sum_{i=1}^n x_i & \sum_{i=1}^n x_i^2 & \sum_{i=1}^n x_i^3 \\ \sum_{i=1}^n x_i^2 & \sum_{i=1}^n x_i^3 & \sum_{i=1}^n x_i^4 \end{bmatrix} \begin{bmatrix} a_0 \\ a_1 \\ a_2 \end{bmatrix} = \begin{bmatrix} \sum_{i=1}^n y_i \\ \sum_{i=1}^n y_i x_i \\ \sum_{i=1}^n y_i x_i^2 \end{bmatrix} \quad (3.1.5)$$

For polynomial degree $m = 3$, from the system of equations (3.1.3), we get the system of the least-squares cube as

$$\begin{bmatrix} n & \sum_{i=1}^n x_i & \sum_{i=1}^n x_i^2 & \sum_{i=1}^n x_i^3 \\ \sum_{i=1}^n x_i & \sum_{i=1}^n x_i^2 & \sum_{i=1}^n x_i^3 & \sum_{i=1}^n x_i^4 \\ \sum_{i=1}^n x_i^2 & \sum_{i=1}^n x_i^3 & \sum_{i=1}^n x_i^4 & \sum_{i=1}^n x_i^5 \\ \sum_{i=1}^n x_i^3 & \sum_{i=1}^n x_i^4 & \sum_{i=1}^n x_i^5 & \sum_{i=1}^n x_i^6 \end{bmatrix} \begin{bmatrix} a_0 \\ a_1 \\ a_2 \\ a_3 \end{bmatrix} = \begin{bmatrix} \sum_{i=1}^n y_i \\ \sum_{i=1}^n y_i x_i \\ \sum_{i=1}^n y_i x_i^2 \\ \sum_{i=1}^n y_i x_i^3 \end{bmatrix} \quad (3.1.6)$$

3.2 Multiple Linear Least-Square Fitting

The multiple linear least-square fitting use linear multi-variables function $Y = a_0 + a_1x + a_2x_2 + \dots + a_\rho x_\rho$, to approximate the given set of data, $(x_{11}, x_{21}, \dots, x_{\rho 1}, y_1)$, $(x_{12}, x_{22}, \dots, x_{\rho 2}, y_2)$, $\dots, (x_{1n}, x_{2n}, \dots, x_{\rho n}, y_n)$. This requires choosing the coefficients a_0, a_1, \dots, a_ρ to minimize the total least square error defined as

$$E = \sum_{i=1}^n (y_i - a_0 - a_1x_{1i} - a_2x_{2i} - \dots - a_\rho x_{\rho i})^2 \quad (3.2.1)$$

To minimize E , a_0, a_1, \dots, a_ρ must satisfy

$$\frac{\partial}{\partial b_j} \left[\sum_{i=1}^n (y_i - b_0 - b_1x_{1i} - b_2x_{2i} - \dots - b_\rho x_{\rho i})^2 \right] = 0 \quad (3.2.2)$$

for $j = 1, 2, \dots, \rho$.

We then obtain

$$\begin{bmatrix} \sum_{i=1}^n 1 & \sum_{i=1}^n x_{1i} & \sum_{i=1}^n x_{2i} & \dots & \sum_{i=1}^n x_{\rho i} \\ \sum_{i=1}^n x_{1i} & \sum_{i=1}^n x_{1i}x_{1i} & \sum_{i=1}^n x_{2i}x_{1i} & \dots & \sum_{i=1}^n x_{\rho i}x_{1i} \\ \sum_{i=1}^n x_{2i} & \sum_{i=1}^n x_{1i}x_{2i} & \sum_{i=1}^n x_{2i}x_{2i} & \dots & \sum_{i=1}^n x_{\rho i}x_{2i} \\ \dots & \dots & \dots & \dots & \dots \\ \sum_{i=1}^n x_{\rho i} & \sum_{i=1}^n x_{1i}x_{\rho i} & \sum_{i=1}^n x_{2i}x_{\rho i} & \dots & \sum_{i=1}^n x_{\rho i}x_{\rho i} \end{bmatrix} \begin{bmatrix} a_0 \\ a_1 \\ a_2 \\ \dots \\ a_\rho \end{bmatrix} = \begin{bmatrix} \sum_{i=1}^n y_i \\ \sum_{i=1}^n y_i x_{1i} \\ \sum_{i=1}^n y_i x_{2i} \\ \dots \\ \sum_{i=1}^n y_i x_{\rho i} \end{bmatrix}. \quad (3.2.3)$$

For the two variables linear function $z = a_0 + a_1x + a_2y$, from the above system of equations, we get the system of the least-squares line as

$$\begin{bmatrix} \sum_{i=1}^n 1 & \sum_{i=1}^n x_i & \sum_{i=1}^n y_i \\ \sum_{i=1}^n x_i & \sum_{i=1}^n x_i x_i & \sum_{i=1}^n y_i x_i \\ \sum_{i=1}^n y_i & \sum_{i=1}^n x_i y_i & \sum_{i=1}^n y_i y_i \end{bmatrix} \begin{bmatrix} a_0 \\ a_1 \\ a_2 \end{bmatrix} = \begin{bmatrix} \sum_{i=1}^n z_i \\ \sum_{i=1}^n z_i x_i \\ \sum_{i=1}^n z_i y_i \end{bmatrix}. \tag{3.2.4}$$

3.3 Nonlinear Least-Squares Fitting

3.3.1 General Method

The least-squares fitting for nonlinear function in terms of chosen coefficients $y = f(x, \theta)$, where $\theta = (\theta_1, \theta_2, \dots, \theta_p)$ is vector of the coefficients. The sum of squared errors is given by

$$E = \sum_{i=1}^n [y_i - f(x_i, \theta)]^2 \tag{3.3.1.1}$$

There are several methods for finding the least squares approximation. The method most often used in computational field is Gauss-Newton method.

For Gauss-Newton method (Myers, 1986), expanding the nonlinear function in a Taylor series around $\theta^{(0)} = (\theta_1^{(0)}, \theta_2^{(0)}, \dots, \theta_p^{(0)})$, and considering only linear terms, we get

$$\begin{aligned} f(x_i, \theta) \approx & f(x_i, \theta^{(0)}) + (\theta_1 - \theta_1^{(0)}) \left[\frac{\partial}{\partial \theta_1} f(x_i, \theta) \right]_{\theta=\theta^{(0)}} \\ & + (\theta_2 - \theta_2^{(0)}) \left[\frac{\partial}{\partial \theta_2} f(x_i, \theta) \right]_{\theta=\theta^{(0)}} \\ & + \dots + (\theta_p - \theta_p^{(0)}) \left[\frac{\partial}{\partial \theta_p} f(x_i, \theta) \right]_{\theta=\theta^{(0)}} \end{aligned} \tag{3.3.1.2}$$

We can write the approximation (3.3.2) as

$$f(x_i, \theta) - f(x_i, \theta^{(0)}) \approx \gamma_1 Q_{1,i} + \gamma_2 Q_{2,i} + \dots + \gamma_p Q_{p,i}, \tag{3.3.1.3}$$

where $Q_{ji} = \left[\frac{\partial}{\partial \theta_j} f(x_i, \theta) \right]_{\theta=\theta^{(0)}}$ and $\gamma_j = \theta_j - \theta_j^{(0)}$.

We now formulate linear multi-variables function of independent variables $\gamma_1, \gamma_2, \dots$ and γ_p as

$$y - f(x, \theta_j^{(0)}) = \gamma_1 Q_1 + \gamma_2 Q_2 + \dots + \gamma_p Q_p. \quad (3.3.1.4)$$

The formulation least-squares fitting can be expressed as

$$\begin{bmatrix} sQQ_{11}^{(0)} & sQQ_{21}^{(0)} & \dots & sQQ_{p1}^{(0)} \\ sQQ_{12}^{(0)} & sQQ_{22}^{(0)} & \dots & sQQ_{p2}^{(0)} \\ \vdots & \vdots & \ddots & \vdots \\ sQQ_{1p}^{(0)} & sQQ_{2p}^{(0)} & \dots & sQQ_{pp}^{(0)} \end{bmatrix} \begin{bmatrix} \gamma_1^{(0)} \\ \gamma_2^{(0)} \\ \vdots \\ \gamma_p^{(0)} \end{bmatrix} = \begin{bmatrix} seQ_1^{(0)} \\ seQ_2^{(0)} \\ \vdots \\ seQ_p^{(0)} \end{bmatrix}, \quad (3.3.1.5)$$

$$seQ_j^{(0)} = \sum_{i=1}^n [y_i - f(x_i, \theta_r)] Q_{ji}^{(0)} \quad (3.3.1.6)$$

and

$$sQQ_{st}^{(0)} = \sum_{i=1}^n Q_{si}^{(0)} Q_{ti}^{(0)} \quad (3.3.1.7)$$

We use an iterative process to approximate θ , using the initial value θ_0 the approximation at the r^{th} iteration, $\theta^{(r)} = (\theta_1^{(r)}, \theta_2^{(r)}, \dots, \theta_p^{(r)})$, is

$$\theta^{(r)} = \theta^{(r-1)} + \gamma^{(r-1)} \quad (3.3.1.8)$$

Continue the process until convergence is reached (the sum of squares and the parameter estimates are no longer changing). In some problems, convergence is very slowly reached. There are several some modifications to reduce calculations or improve convergence.

Use of fractional increments, the iteration can be modified as:

1. Compute θ_r from the equation (3.3.1.8) and

$$E^{(r)} = \sum_{i=1}^n [y_i - f(x_i, \theta^{(r)})]^2 \quad (3.3.1.9)$$

2. If $E^{(r)} > E^{(r-1)}$, re-compute

$$\theta^{(r)} = \theta^{(r-1)} + \frac{\gamma^{(r-1)}}{2}. \tag{3.3.1.10}$$

3.3.2 Linearization of Nonlinear Least-squares fitting

Consider a function of the form

$$y = ax^b. \tag{3.3.2.1}$$

We can transform this to a linear equation by taking the logarithm of both sides of the equation (3.3.2.1) as

$$\log y = \log a + b \log x. \tag{3.3.2.2}$$

Thus, from the equation (3.1.4), we have

$$\begin{bmatrix} n & \sum_{i=1}^n \log x_i \\ \sum_{i=1}^n \log x_i & \sum_{i=1}^n (\log x_i)^2 \end{bmatrix} \begin{bmatrix} \log a \\ b \end{bmatrix} = \begin{bmatrix} \sum_{i=1}^n \log y_i \\ \sum_{i=1}^n \log y_i \log x_i \end{bmatrix}. \tag{3.3.2.3}$$

3.4 Backpropagation Algorithm

The squared errors of a multilayer neural network is defined as

$$E(w_1, w_2, \dots, w_N) = \sum_{p=1}^P \sum_{k=1}^K (d_{kp} - o_{kp})^2, \tag{3.4.1}$$

where w_1, w_2, \dots, w_N are weights of the neural network, d_{kp} is the desired (target) value of the k^{th} output neuron and the p^{th} pattern, o_{kp} is the computed value of the k^{th} output neuron and the p^{th} pattern, N is the number of weights, P is the number of patterns, and K is the number of output neurons. For a two-layer neural network we define the squared errors as

$$\begin{aligned} E(w_{11}, \dots, w_{1H}, w_{21}, \dots, w_{2H}, \dots, w_{I1}, \dots, w_{IH}, \\ v_{11}, \dots, v_{1K}, v_{21}, \dots, v_{2K}, \dots, v_{H1}, \dots, v_{HK}) \\ = \sum_{p=1}^P \sum_{k=1}^K (d_{kp} - o_{kp})^2 \end{aligned}, \tag{3.4.2}$$

where w_{ih} is the weight from the i^k input neuron to the h^{th} hidden neuron, v_{hk} is the weight from the h^{th} hidden neuron to the k^{th} output neuron, I is the number of input neurons and H is the number of hidden neurons.

We rewrite the Eq. (3.4.2) as

$$E = \sum_{p=1}^P \sum_{k=1}^K [d_{kp} - f_2(\sum_{h=1}^H v_{hk} f_1(\sum_{i=1}^I w_{ih} INP_{ip})))]^2, \quad (3.4.3)$$

where f_1 and f_2 are activation functions of a neuron in the hidden layer and out put layer, and INP_{ip} is the value of the i^k input neuron and the p^{th} pattern.

Backpropagation (Rumelhart, 1986) is a technique to minimize some error criteria E . Using backpropagation with a two-layer neural network, weights update can be expressed as

$$w_{ih}^{(r+1)} = w_{ih}^{(r)} - \eta \frac{\partial E}{\partial w_{ih}} + \alpha (w_{ih}^{(r)} - w_{ih}^{(r-1)}) \quad (3.4.4)$$

and

$$v_{hk}^{(r+1)} = v_{hk}^{(r)} - \eta \frac{\partial E}{\partial v_{hk}} + \alpha (v_{hk}^{(r)} - v_{hk}^{(r-1)}), \quad (3.4.5)$$

where $w_{ih}^{(r)}$ is the weight w_{ih} in the r^{th} step, $v_{hk}^{(r)}$ is the weight v_{hk} in the r^{th} step, η and α are parameters called learning rate and momentum, respectively.

We can express the partial derivatives in the Eqs. (3.4.4) and (3.4.5) as

$$\frac{\partial E}{\partial v_{hk}} = -2(d_{kp} - o_{kp}) f_2' f_1' \left(\sum_{i=1}^I w_{ih} INP_{ip} \right) \quad (3.4.6)$$

and

$$\frac{\partial E}{\partial w_{ih}} = -2 \sum_{k=1}^K (d_{kp} - o_{kp}) f_2' v_{hk} f_1' INP_{ip}, \quad (3.4.7)$$

where $f_1' = \left. \frac{df_1(z)}{dz} \right|_{z = \sum_{i=1}^I w_{ih} INP_{ip}}$ and $f_2' = \left. \frac{df_2(z)}{dz} \right|_{z = \sum_{h=1}^H v_{hk} f_1' \left(\sum_{i=1}^I w_{ih} INP_{ip} \right)}$.

3.5 Performance Measurement

In this work, we use relative root mean square error (RMSE) and bias (BIAS) to measure performance of the model involved into forecasting is estimated in terms of, computed as

$$RMSE = \sqrt{\frac{\sum_{i=1}^n [(y_i - x_i) / y_i]^2}{n}} \quad (3.5.1)$$

$$BIAS = \frac{\sum_{i=1}^n (y_i - x_i) / y_i}{n} \quad (3.5.2)$$

where y_i is the i^{th} observed value, x_i is the i^{th} predicted value and n is number of all values in a set of data.

CHAPTER IV

EXPERIMENTS AND RESULTS

4.1 Data

The wind and wave data are from the UNOCAL buoy station, location at 101.43° E and 9.26° N, shown in Figure 4.1.1. Generally, the data are recorded in each 20 minutes on everyday. However, we get some data not continuously recorded in the step of time 20 minutes. Then we try to select data of some ranges continuously recorded in the time step as long as. We select that data in year 1995, 1996, 1997 and 1998 and fit the parametric models.

The data used in this research consist of :

- (1) The data in 15 January 1995 to 3 March 1995, this data contain 26 samples,
- (2) The data in 25 August 1995 to 25 September 1995, this data contain 2245 samples,
- (3) The data in 22 August 1996 to 20 September 1996, this data contain 2134 samples,
- (4) The data in 8 December 1996 to 31 December 1996, this data contain 1719 samples,
- (5) The data in 18 August 1997 to 25 August 1997, this data contain 531 samples,
- (6) The data in 2 December 1997 to 28 December 1997, this data contain 1921 samples and
- (7) The data in 17 March 1998 to 8 April 1998, this data contain 1656 samples.

We call these data that the all of the selected data, this data contain 12878 samples.

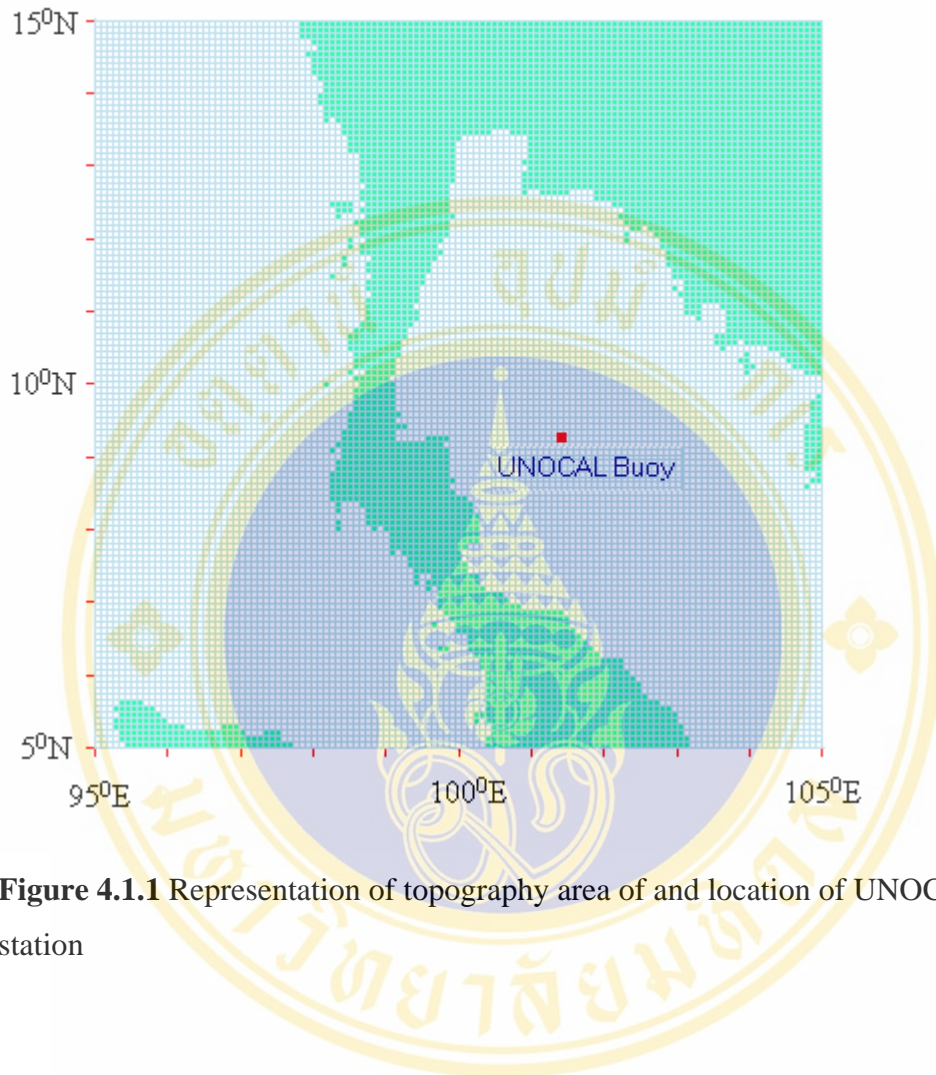


Figure 4.1.1 Representation of topography area of and location of UNOCAL buoy station

4.2 Experiments

First we try to plot wind speed and direction, fetch, significant wave height and significant wave period in time, which is shown in Figure 4.2.1.

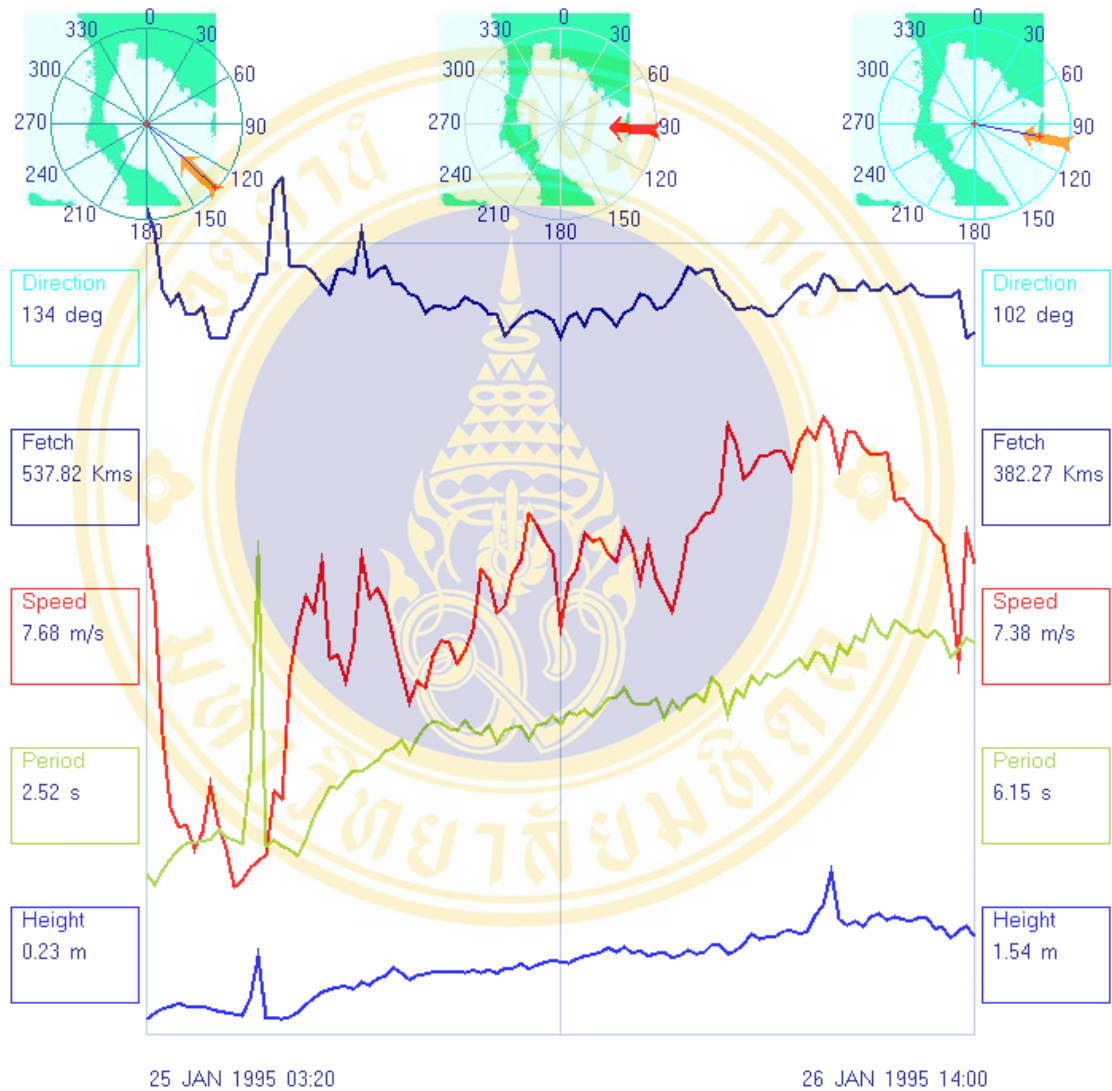


Figure 4.2.1 Wave parameters plots in time

Then we try to see the direction of wind from the selected data, these agree with northeast monsoon and southwest monsoon as shown in Figure 4.2.2 to Figure 4.2.8.

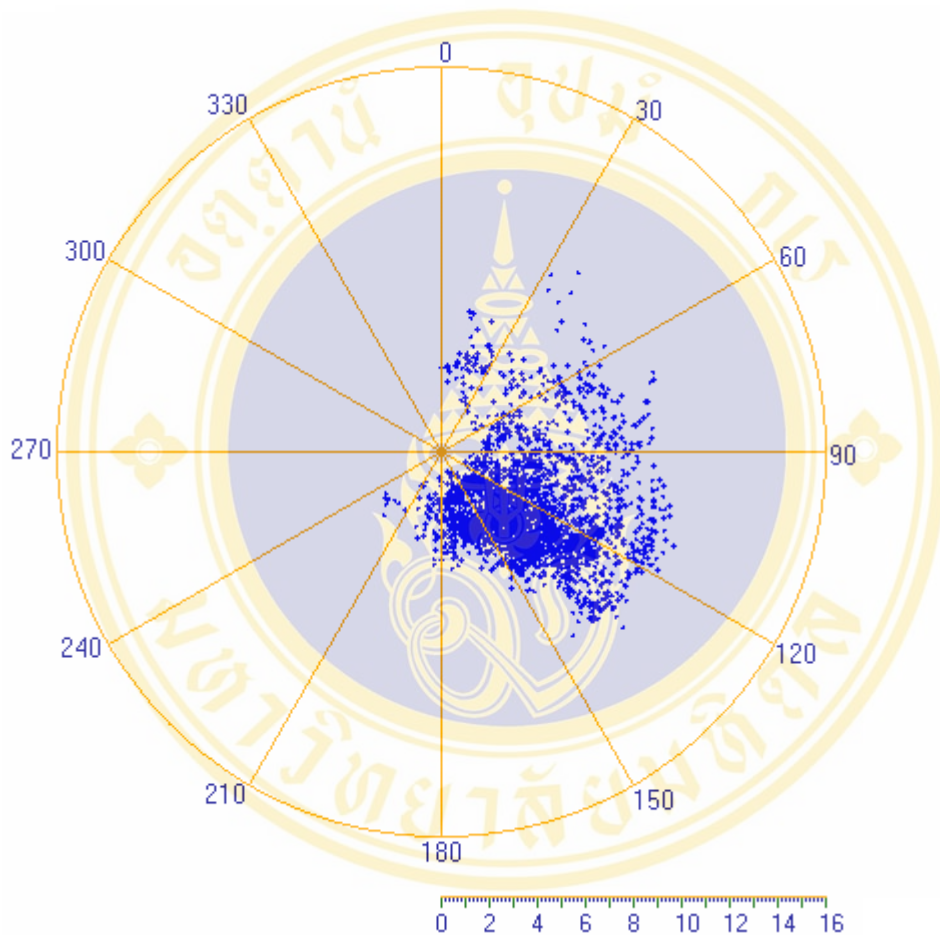


Figure 4.2.2 Scatter plots of speed and direction of wind in 15 January 1995 to 3 March 1995, the data nearly represents northeast monsoon

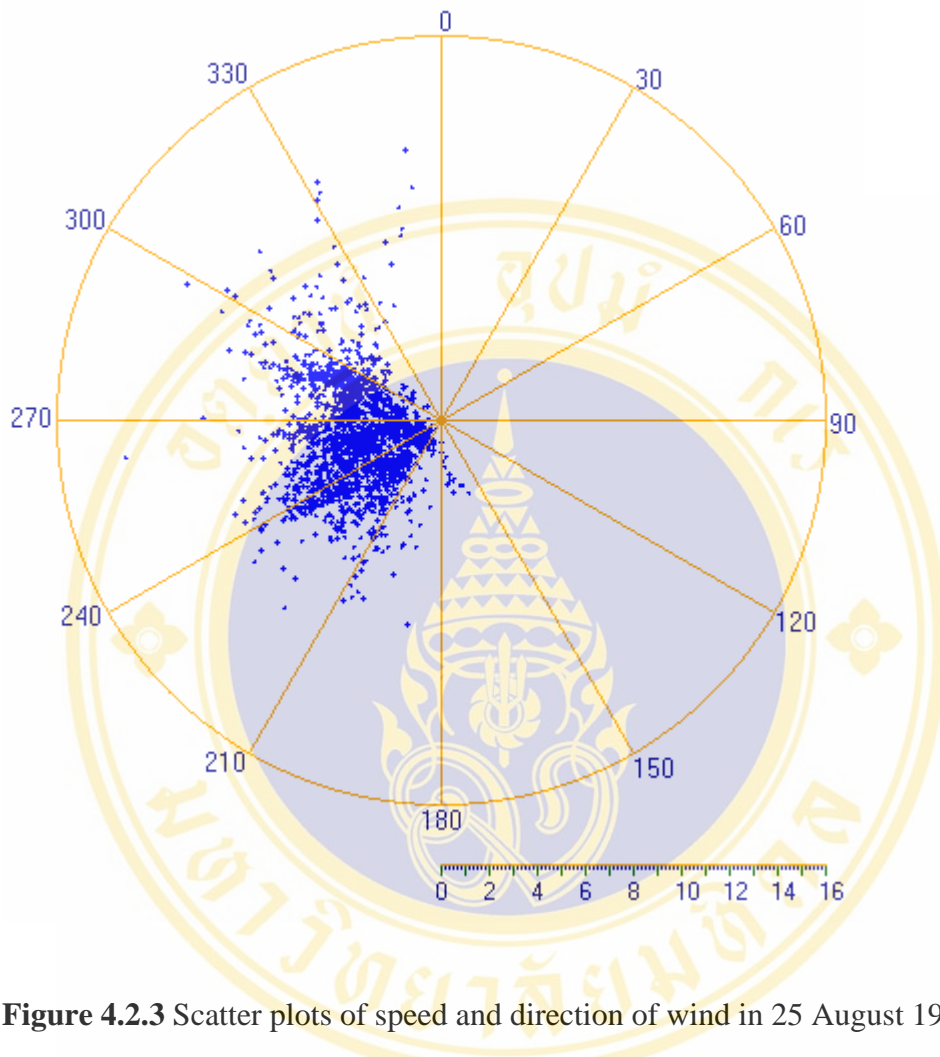


Figure 4.2.3 Scatter plots of speed and direction of wind in 25 August 1995 to 25 September 1995, the data nearly represents southwest monsoon

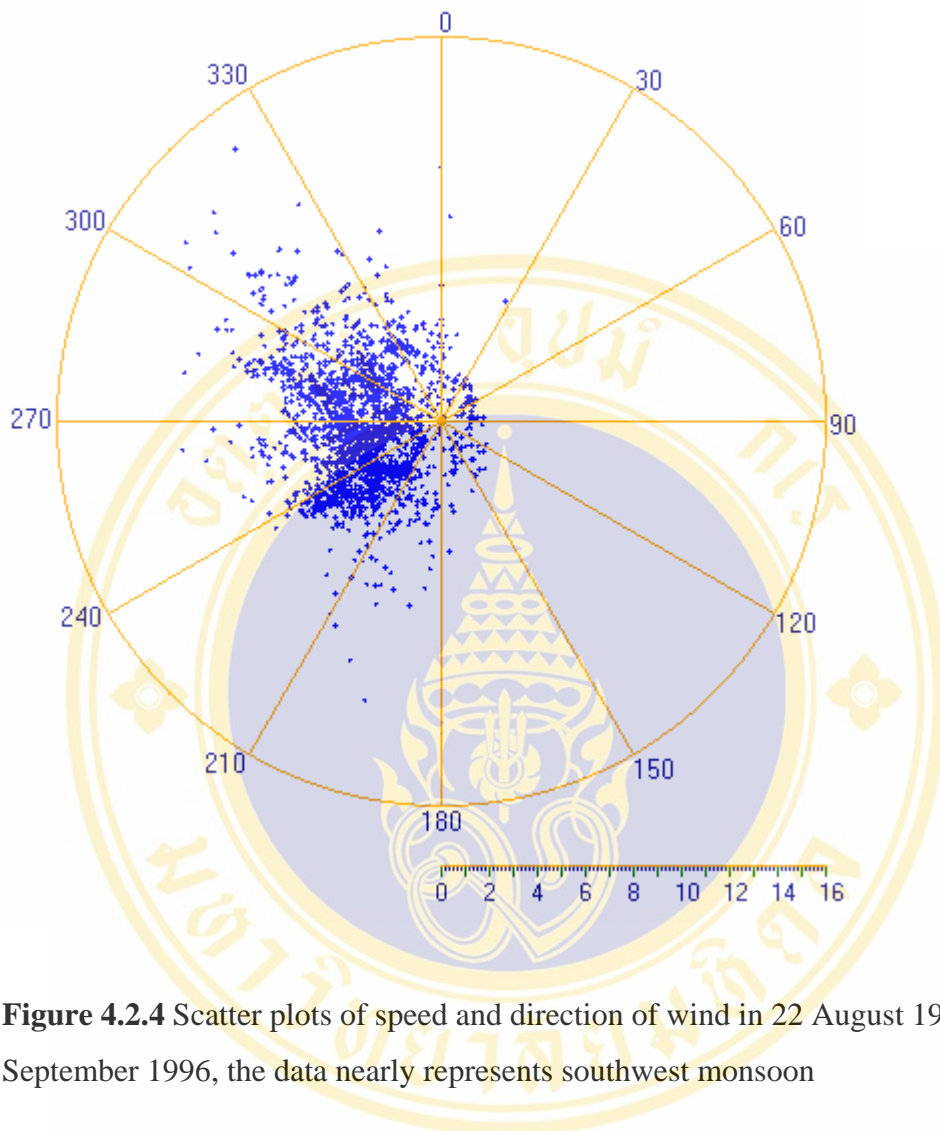


Figure 4.2.4 Scatter plots of speed and direction of wind in 22 August 1996 to 20 September 1996, the data nearly represents southwest monsoon

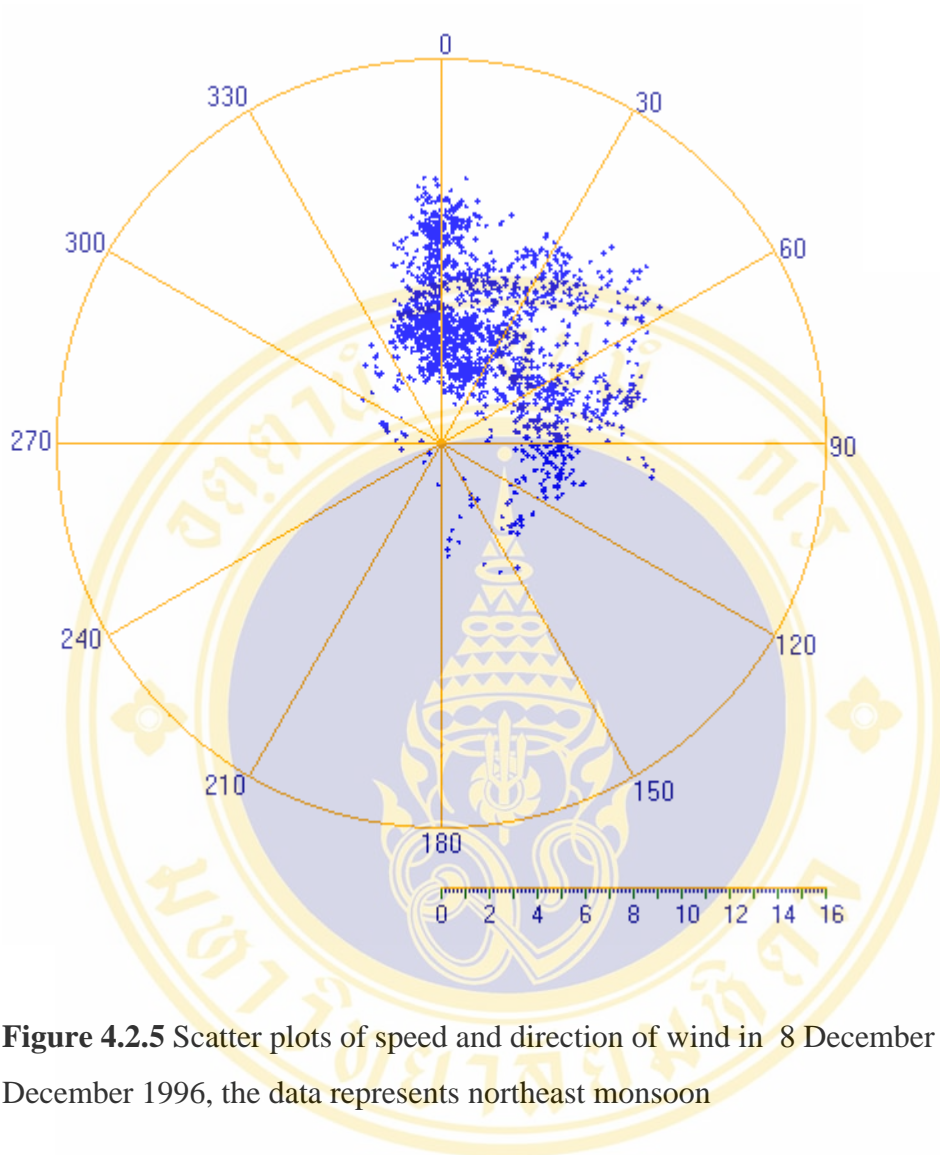


Figure 4.2.5 Scatter plots of speed and direction of wind in 8 December 1996 to 31 December 1996, the data represents northeast monsoon

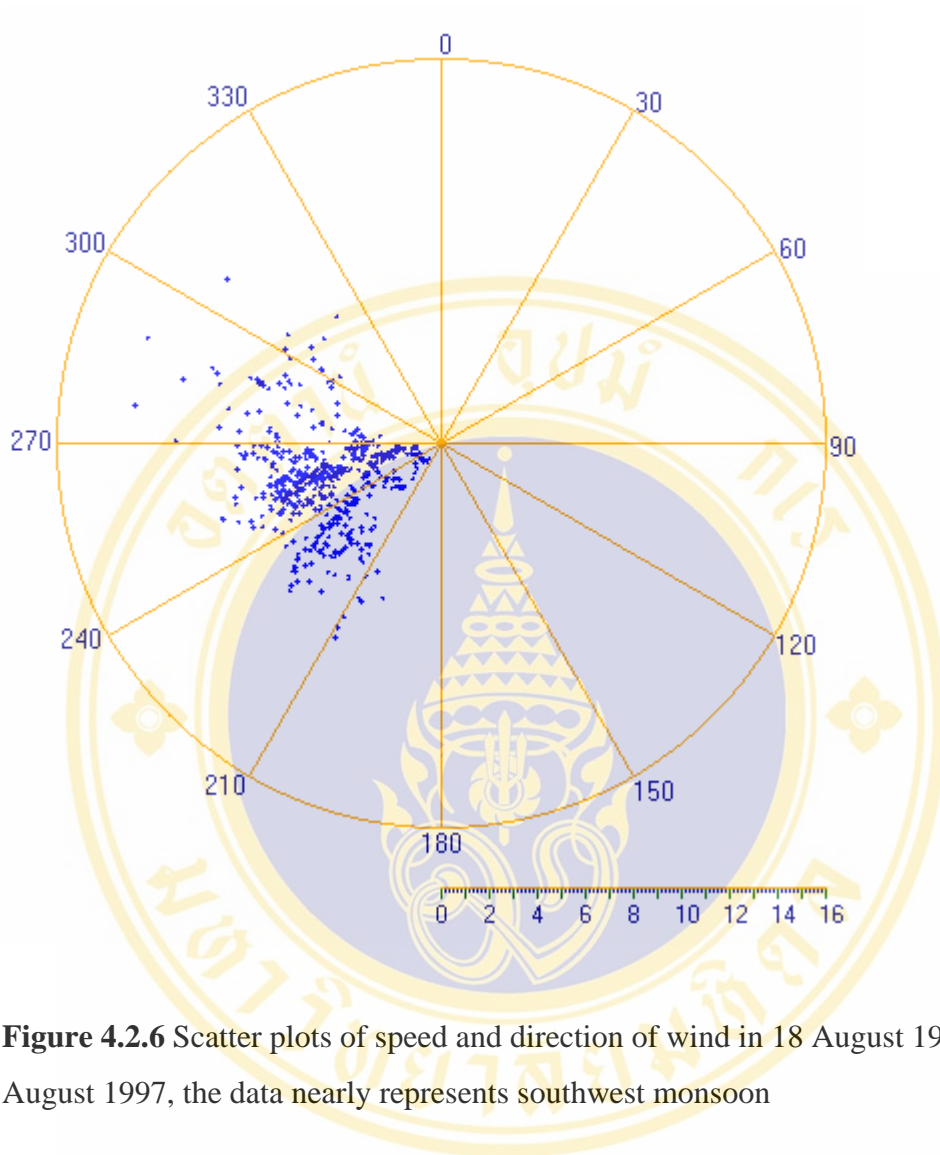


Figure 4.2.6 Scatter plots of speed and direction of wind in 18 August 1997 to 25 August 1997, the data nearly represents southwest monsoon

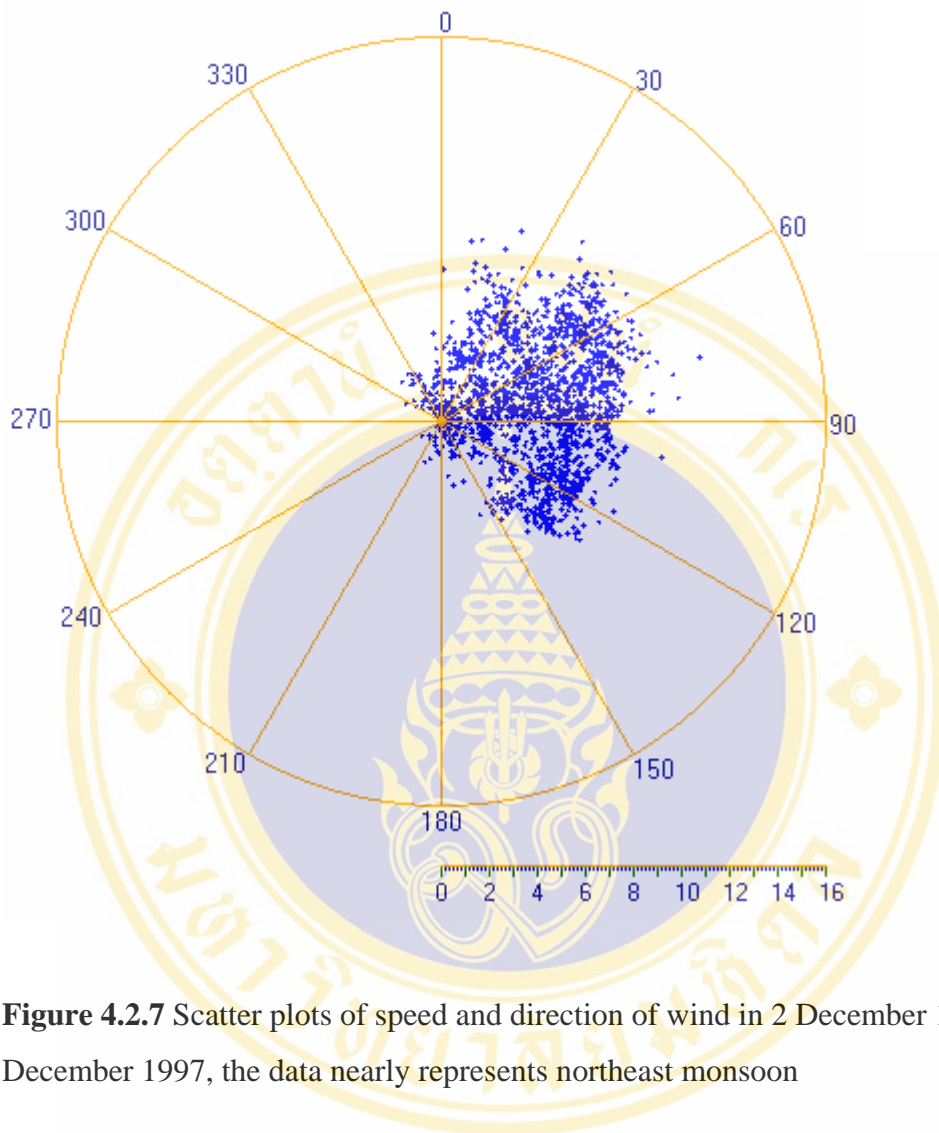


Figure 4.2.7 Scatter plots of speed and direction of wind in 2 December 1997 to 28 December 1997, the data nearly represents northeast monsoon

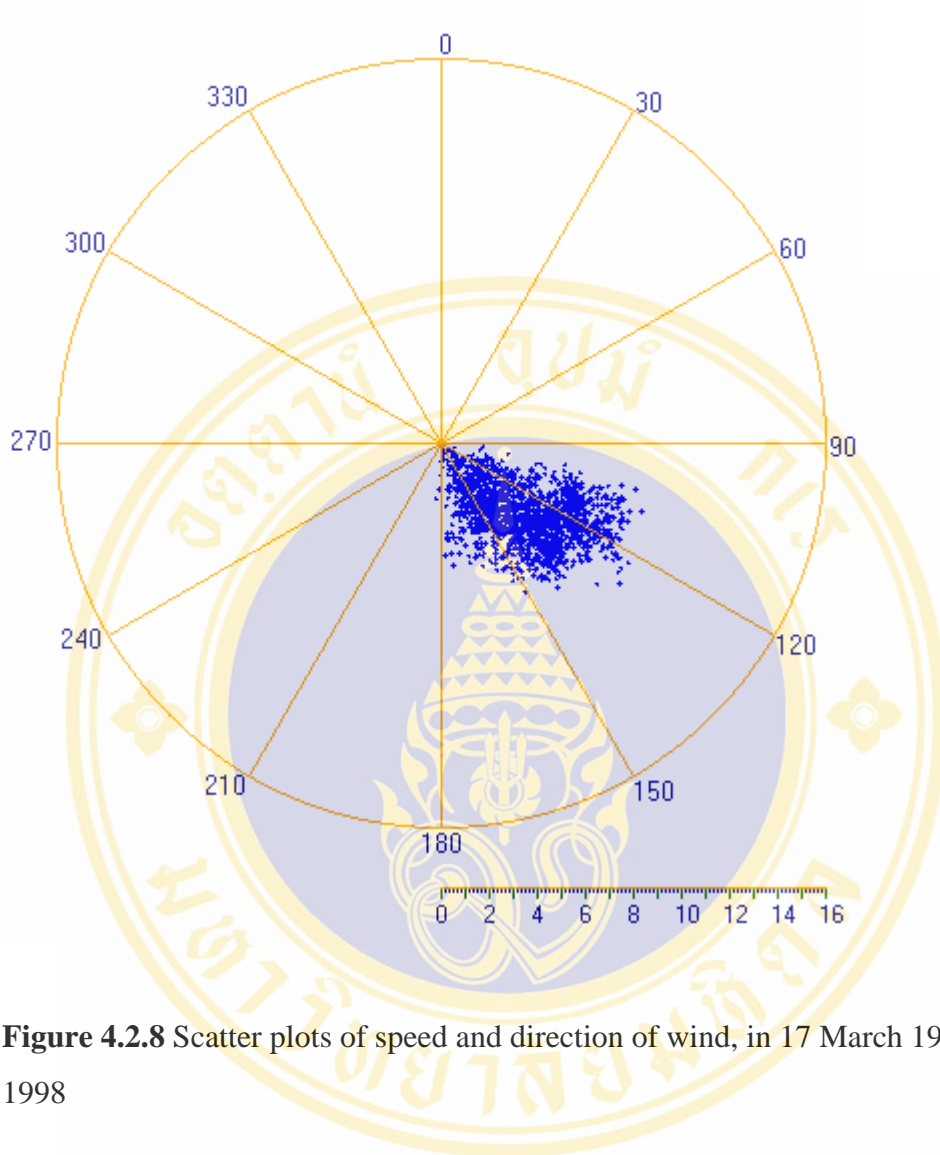


Figure 4.2.8 Scatter plots of speed and direction of wind, in 17 March 1998 to 8 April 1998

The data in 17 March 1998 to 8 April 1998, shown in Figure 4.2.8, is appropriate for finding the fully developed sea condition, since the mean of direction of wind is 132.38 degrees. There are 1656 samples in this data. The mean of the fetch length of the wind is greater than 495 kilometers, shown in Table 4.1. We try to use the least-squares parabola, cube polynomial degree 4 and polynomial degree 5 and nonlinear least-squares with the data.

Table 4.1 Mean of concerned parameters of the data in 17 March 1998 to 8 April 1998

Mean of wind speed	Mean of significant wave height	Mean of significant wave period	Mean of Wind direction	Mean of Fetch length
4.75 m/s	0.93 m	4.75 s	132.41 deg	> 495 km

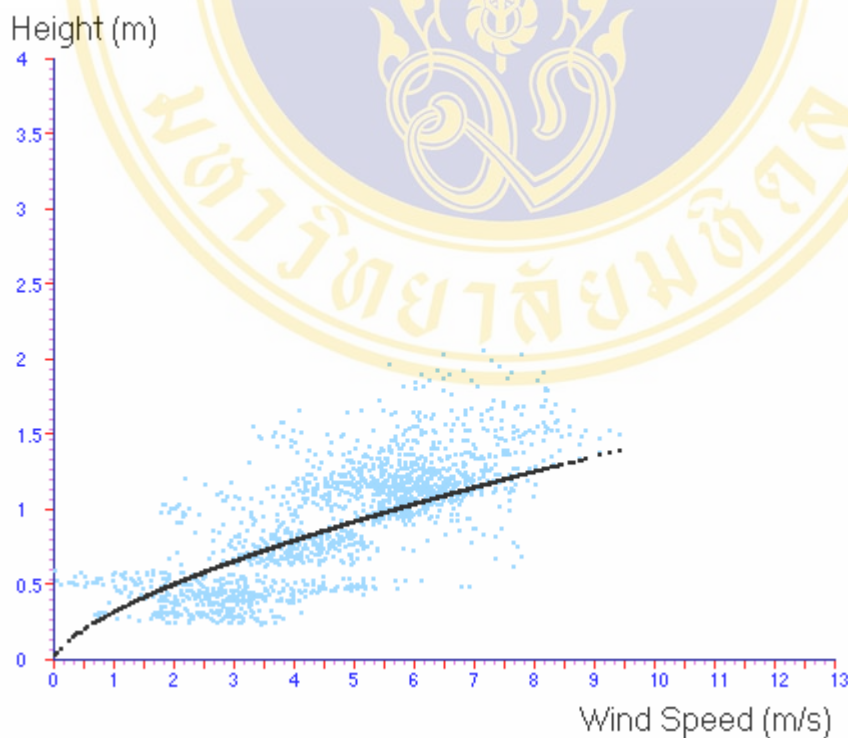


Figure 4.2.9 Scatter plots and curves of nonlinear least-square fits of wind speed and significant wave height in 17 March 1998 to 8 April 1998

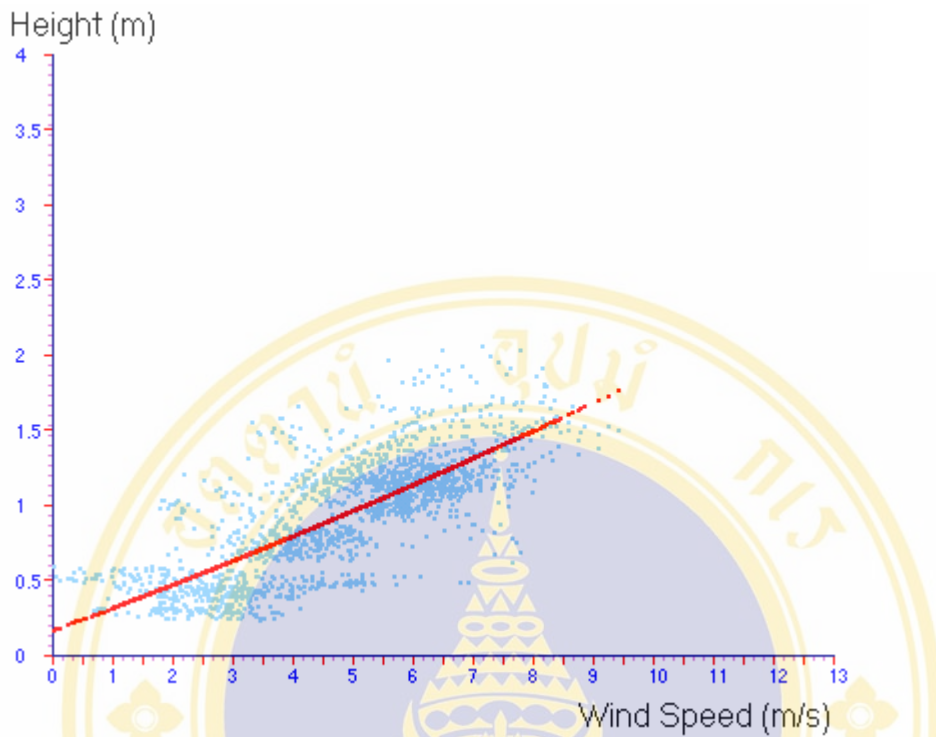


Figure 4.2.10 Scatter plots and curve of least-square parabola of wind speed and significant wave height in 17 March 1998 to 8 April 1998

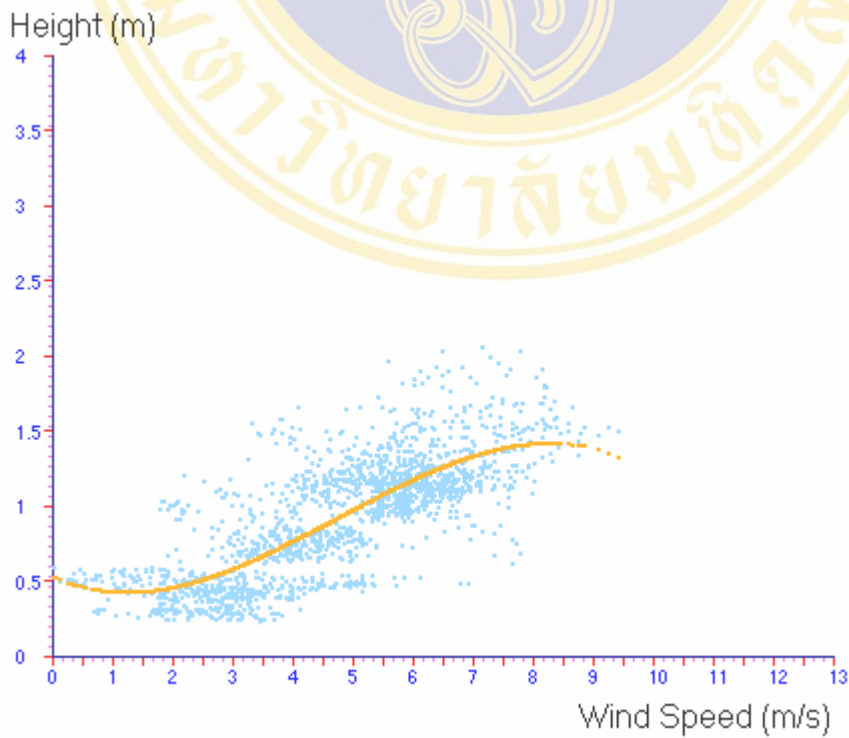


Figure 4.2.11 Scatter plots and curves of least-square cube of wind speed and significant wave height in 17 March 1998 to 8 April 1998

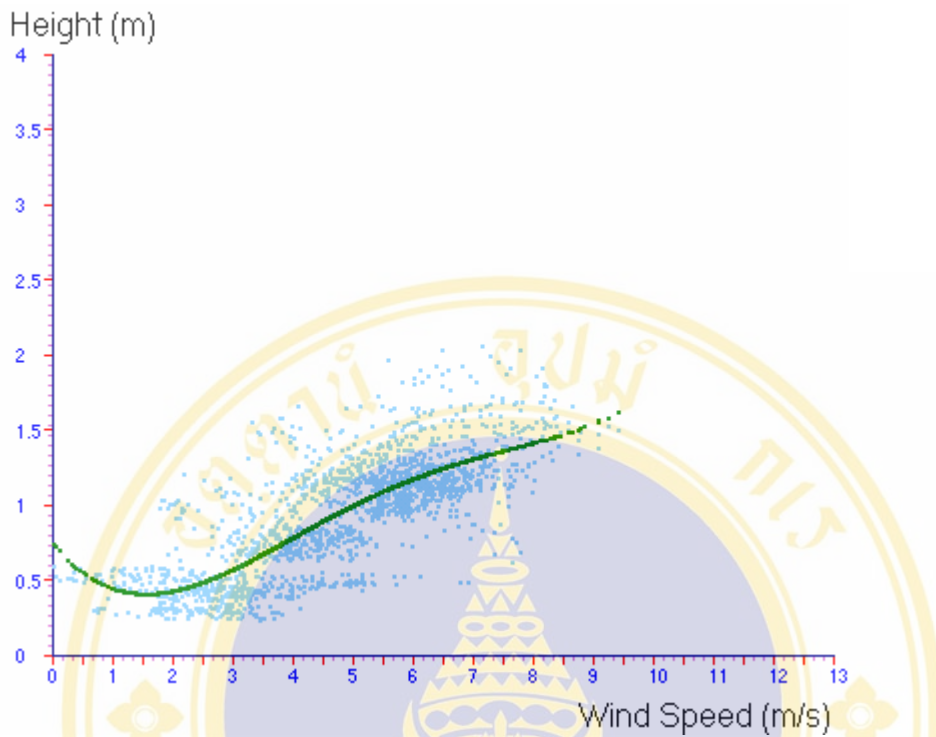


Figure 4.2.12 Scatter plots and curves of least-square polynomial degree 4 of wind speed and significant wave height in 17 March 1998 to 8 April 1998

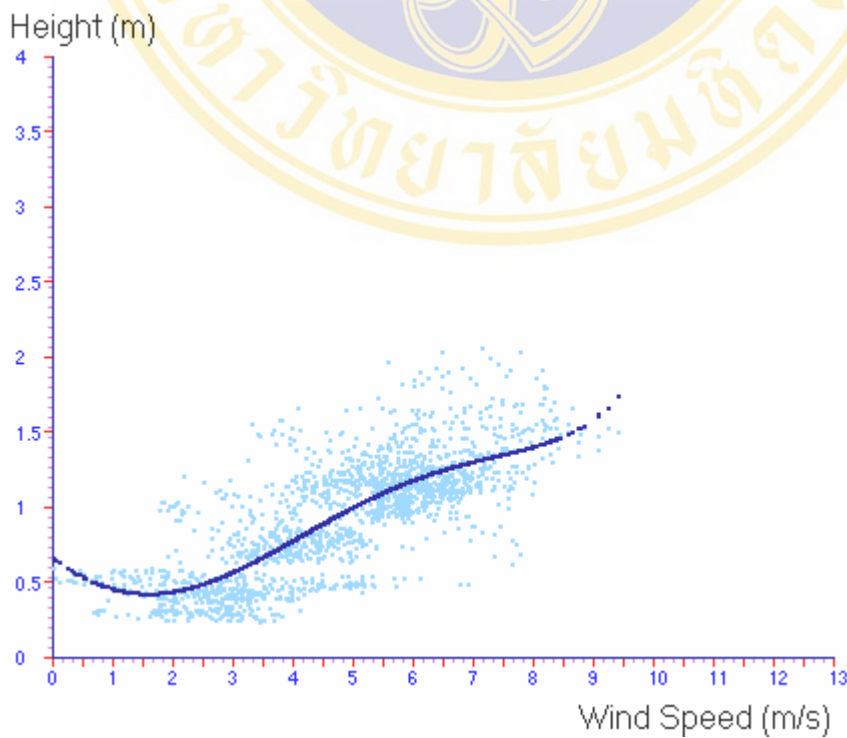


Figure 4.2.13 Scatter plots and curve of least-square polynomial degree 5 of wind speed and significant wave height in 17 March 1998 to 8 April 1998

Table 4.2 Root mean square error (RMSE) and bias (BIAS) of least-square fitting of wind speed and significant wave height of the data in 17 March 1998 to 8 April 1998

Least-square fitting	RMSE	BIAS
Nonlinear	0.4285811	-0.07013582
Parabola	0.4149063	-0.1098001
Cube	0.3824375	-0.1022253
Polynomial degree 4	0.3789222	-0.09929535
Polynomial degree 5	0.3766145	-0.09921043

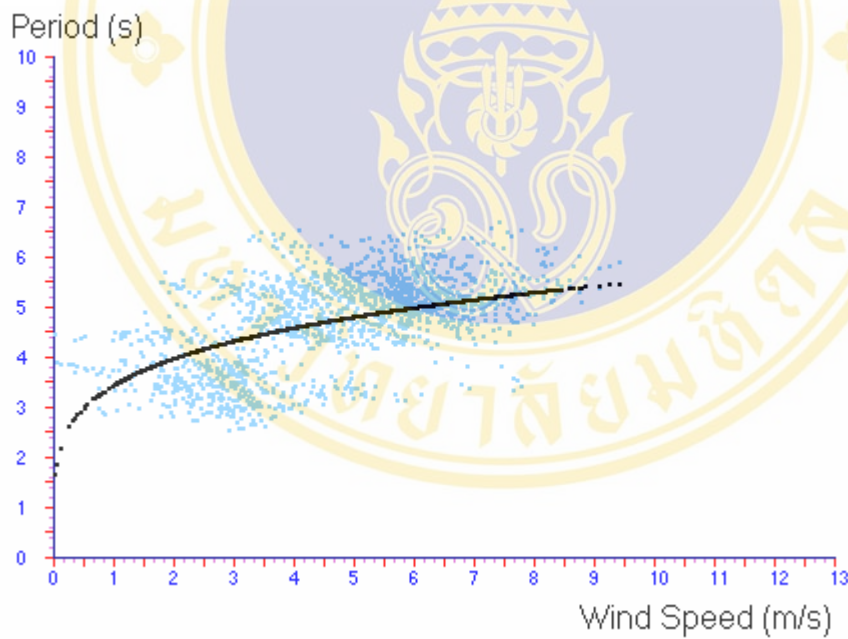


Figure 4.2.14 Scatter plots and curve of nonlinear least-square fits of wind speed and significant wave period in 17 March 1998 to 8 April 1998

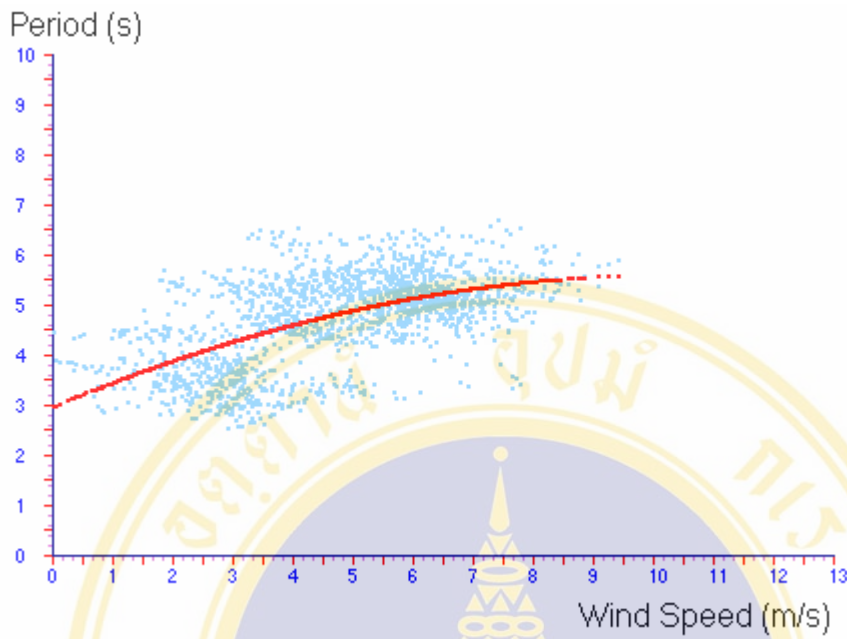


Figure 4.2.15 Scatter plots and curve of least-square parabola of wind speed and significant wave period in 17 March 1998 to 8 April 1998

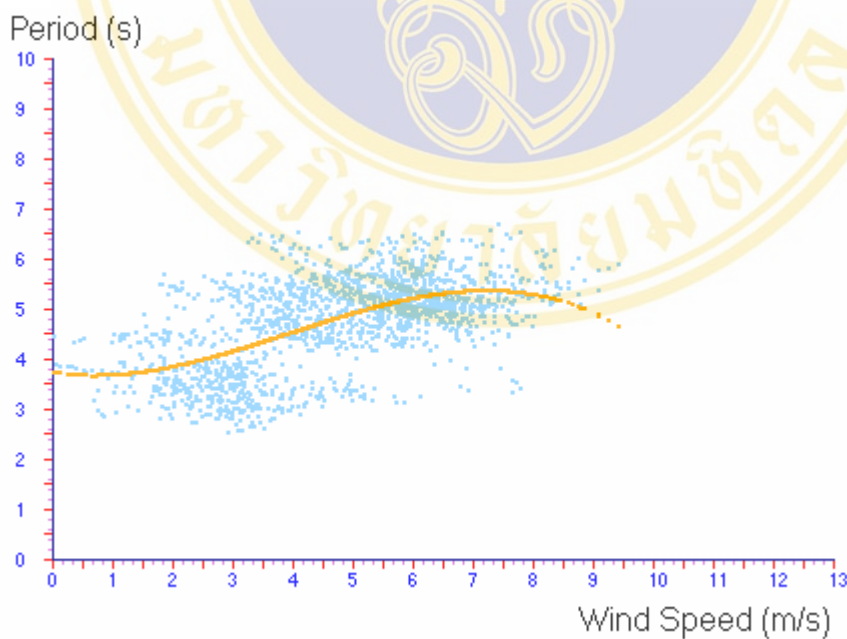


Figure 4.2.16 Scatter plots and curve of least-square cube of wind speed and significant wave period in 17 March 1998 to 8 April 1998

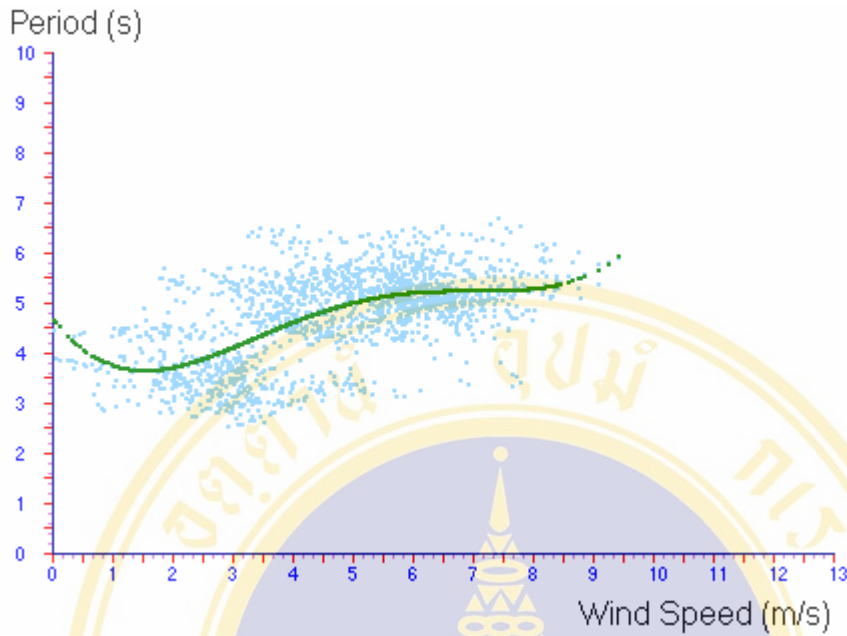


Figure 4.2.17 Scatter plots and curve of least-square polynomial degree 4 of wind speed and significant wave period in 17 March 1998 to 8 April 1998

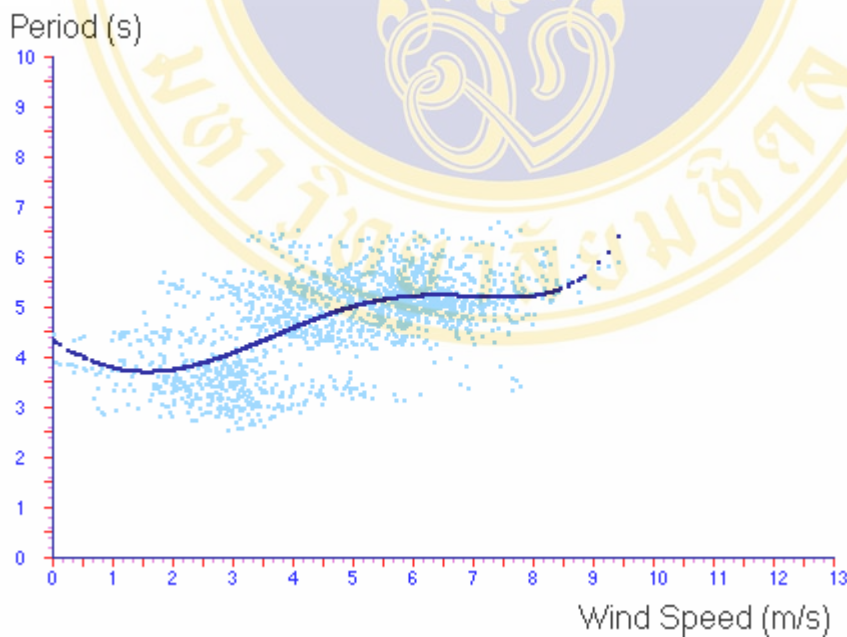


Figure 4.2.18 Scatter plots and curve of least-square polynomial degree 5 of wind speed and significant wave period in 17 March 1998 to 8 April 1998

Table 4.3 Root mean square error (RMSE) and bias (BIAS) of least-square fitting of wind speed and significant wave period of the data in 17 March 1998 to 8 April 1998

Least-square fitting	RMSE	BIAS
Nonlinear	0.1889607	-0.0159858
Parabola	0.1854680	-0.02857035
Cube	0.1801915	-0.02776847
Polynomial degree 4	0.1786510	-0.0270976
Polynomial degree 5	0.1776893	-0.0270096

We see from the Table 4.2 and 4.3 that significant wave height and significant wave period of the data in 17 March 1998 to 8 April 1998, is good fit with high degree polynomial of wind speed. However (WMO, 1995), in generally significant wave height varies roughly as the square of wind speed. From this we choose the case of least of root mean square error (RMSE). The fully developed sea for significant wave height from this data set is given by

$$H_{\infty} = 0.0001526886u^5 - 0.002370412u^4 + 0.002652375u^3 + 0.1030923u^2 - 0.3143224u + 0.6665258 \quad (4.1.1)$$

The fully developed sea for significant wave period from this data set is given by

$$T_{\infty} = 0.0006293007u^5 - 0.009462122u^4 + 0.01658205u^3 + 0.2694033u^2 - 0.8399428u + 4.359134 \quad (4.1.2)$$

We also choose the data of wave height in 25 August 1995 to 25 September 1995 to find wave growth with fetch, since the fetch length of the wind varies in range 170 to 611 kilometers, shown in Table 4.4. There are 2245 samples in this data set. We try to use the least-squares parabola, cube polynomial degree 4 and polynomial degree 5 and nonlinear least-squares with the data, shown in figure 4.20 to 4.29.

Table 4.4 Range of the fetch length of the data in 25 August 1995 to 25 September 1995

Minimum of the fetch length	Mean of the fetch length	Maximum of the fetch length
170.72 km	215.22 km	611.25 km

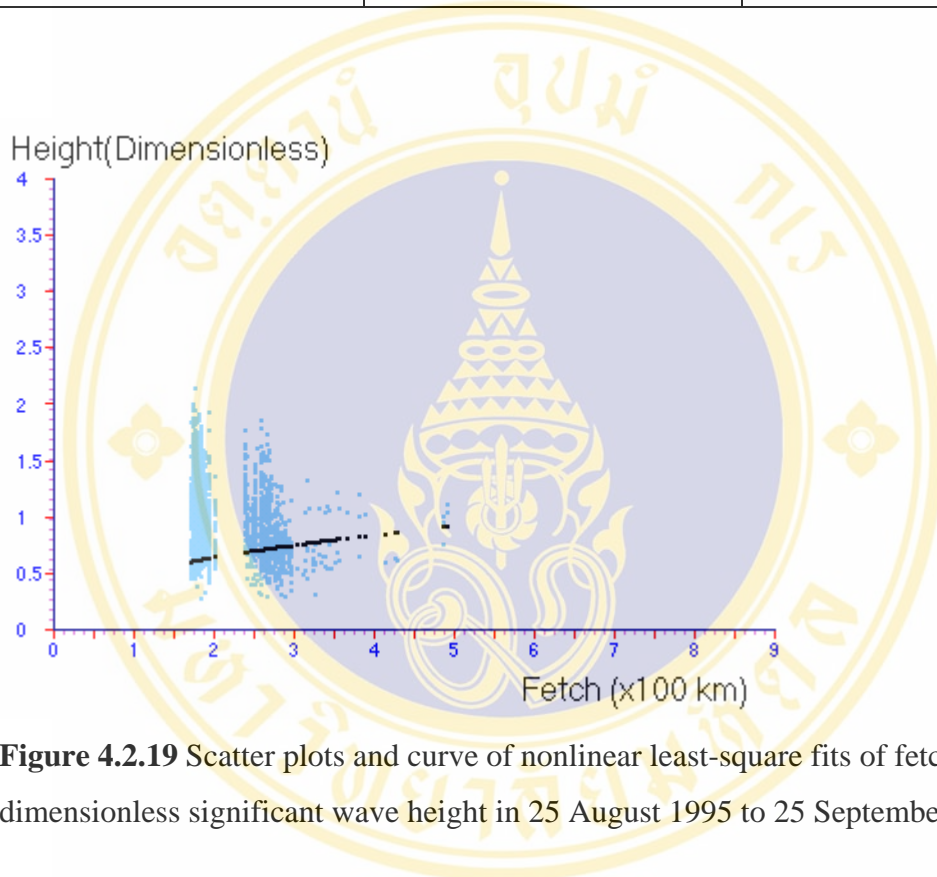


Figure 4.2.19 Scatter plots and curve of nonlinear least-square fits of fetch length and dimensionless significant wave height in 25 August 1995 to 25 September 1995

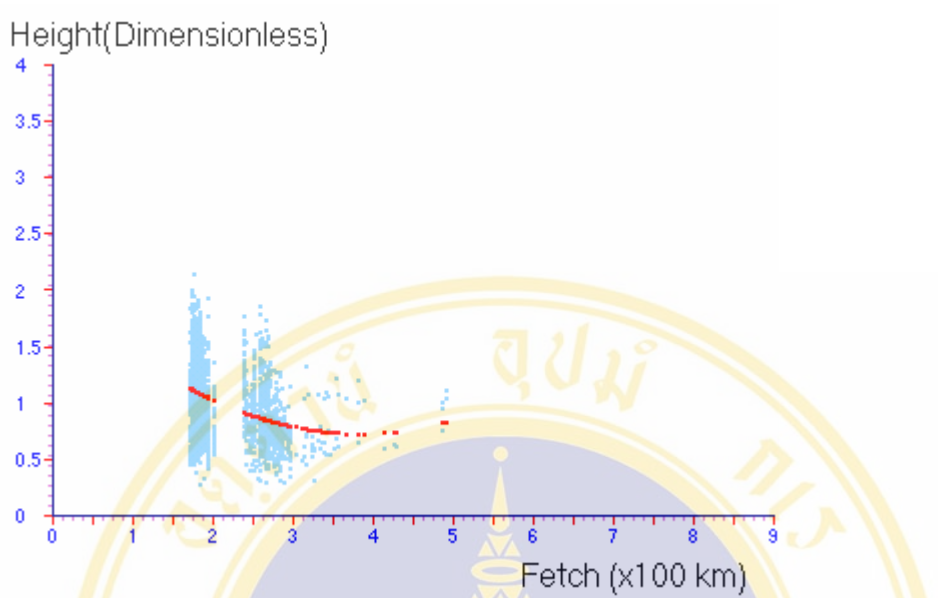


Figure 4.2.20 Scatter plots and curve of least-square parabola fits of fetch length and dimensionless significant wave height in 25 August 1995 to 25 September 1995

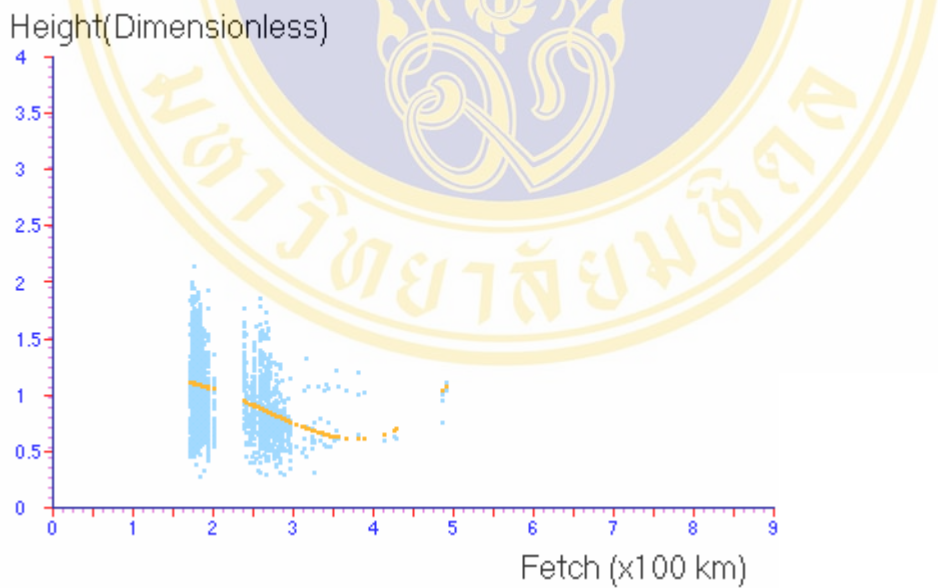


Figure 4.2.21 Scatter plots and curve of least-square parabola fits of fetch length and dimensionless significant wave height in 25 August 1995 to 25 September 1995

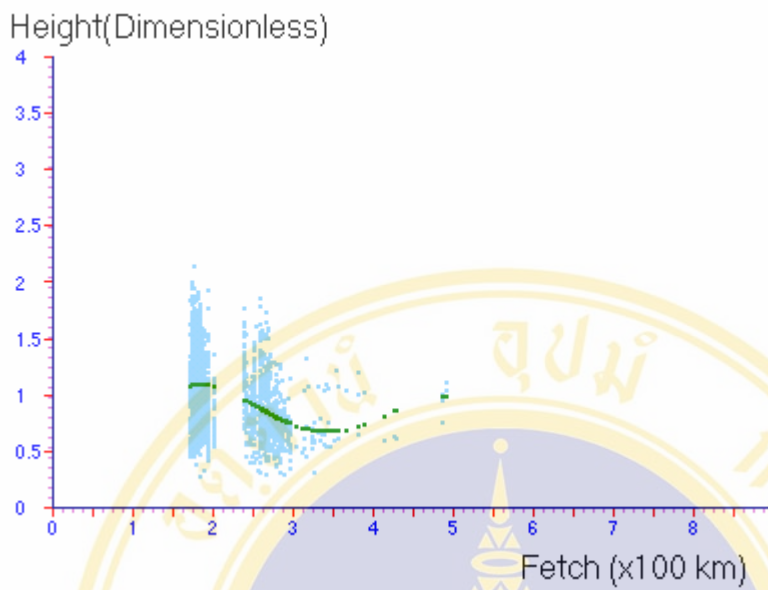


Figure 4.2.22 Scatter plots and curve of least-square polynomial degree 4 fits of fetch length and dimensionless significant wave height in 25 August 1995 to 25 September 1995

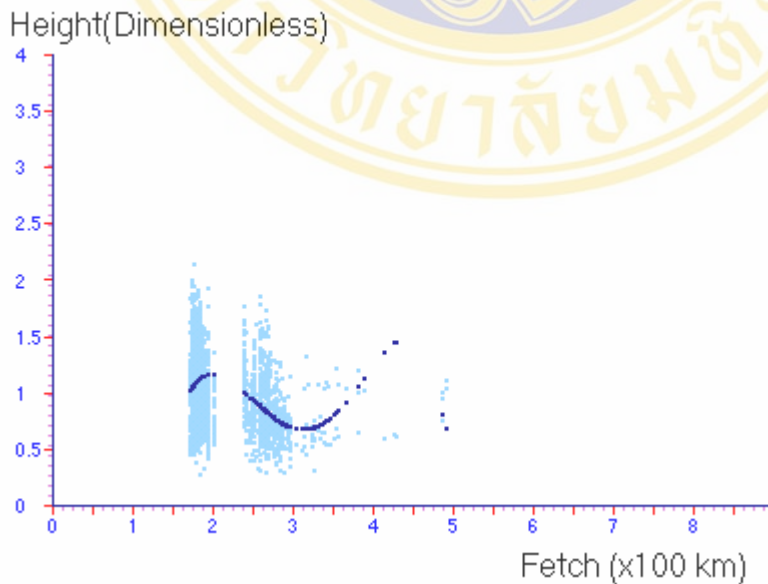


Figure 4.2.23 Scatter plots and curve of least-square polynomial degree 5 fits of fetch length and dimensionless significant wave height in 25 August 1995 to 25 September 1995

Table 4.5 Root mean square error (RMSE) and bias (BIAS) of least-square fitting of the fetch length and dimensionless significant wave height of the data in 25 August 1995 to 25 September 1995

Least-square fitting	RMSE	BIAS
Nonlinear	0.3931282	0.2606752
Parabola	0.3769635	-0.09832741
Cube	0.3751962	-0.09741098
Polynomial degree 4	0.3742383	-0.09697488
Polynomial degree 5	0.3777015	-0.09556292

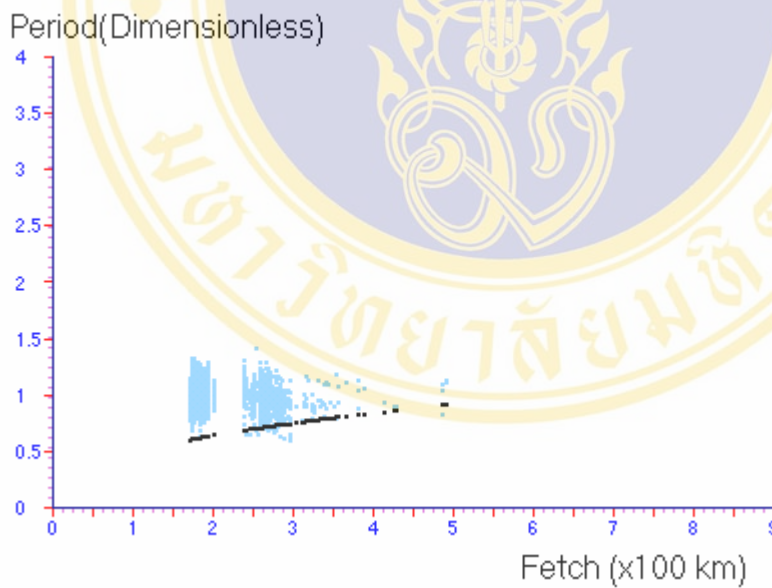


Figure 4.2.24 Scatter plots and curve of nonlinear least-square fits of fetch length and dimensionless significant wave period in 25 August 1995 to 25 September 1995

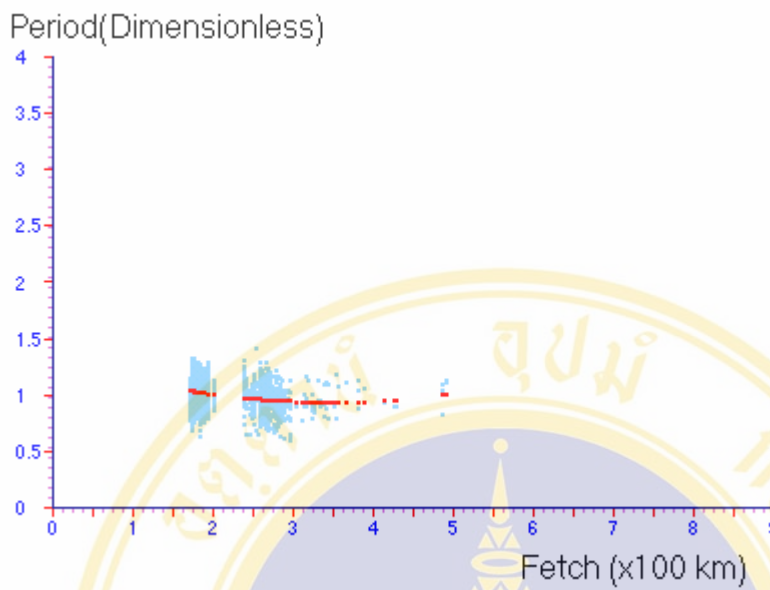


Figure 4.2.25 Scatter plots and curve of least-square parabola fits of fetch length and dimensionless significant wave period in 25 August 1995 to 25 September 1995

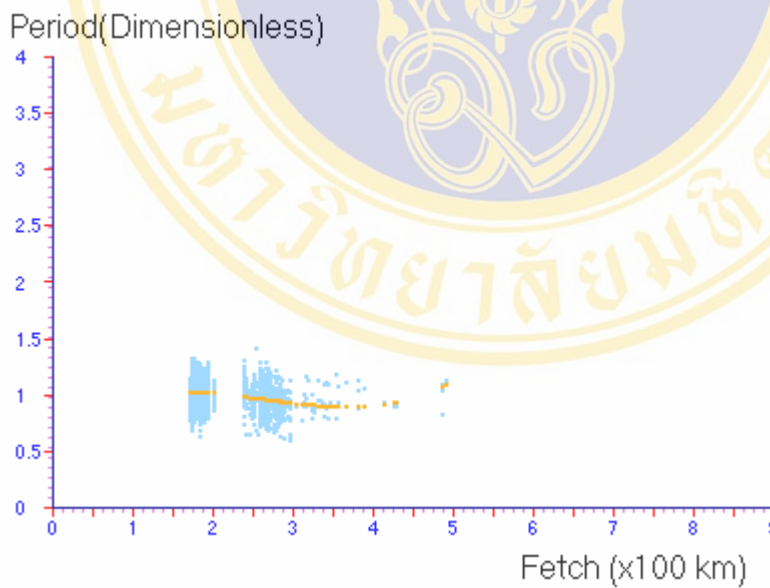


Figure 4.2.26 Scatter plots and curve of least-square cube fits of fetch length and dimensionless significant wave period in 25 August 1995 to 25 September 1995

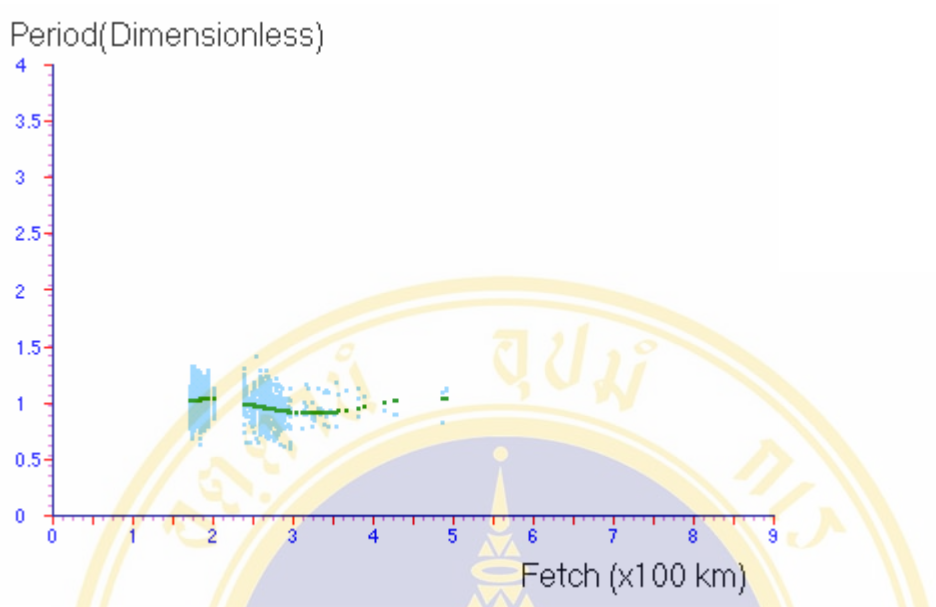


Figure 4.2.27 Scatter plots and curve of least-square polynomial degree 4 fits of fetch length and dimensionless significant wave period in 25 August 1995 to 25 September 1995

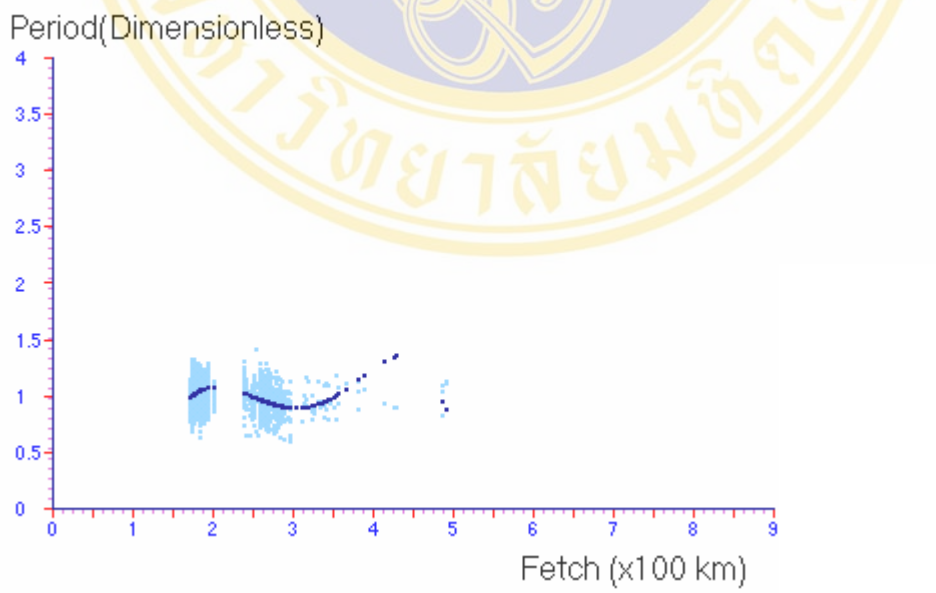


Figure 4.2.28 Scatter plots and curve of least-square polynomial degree 5 fits of fetch length and dimensionless significant wave period in 25 August 1995 to 25 September 1995

Table 4.6 Root mean square error and bias of least-square fitting of fetch length and dimensionless significant wave period of the data period in 25 August 1995 to 25 September 1995

Least-square fitting	RMSE	BIAS
Nonlinear	0.3523077	0.332643
Parabola	0.1266769	-0.01457022
Cube	0.1263311	-0.01449561
Polynomial degree 4	0.1258657	-0.01440088
Polynomial degree 5	0.128162	-0.01410743

We see from the Table 4.2 and 4.3 that dimensionless significant wave height and dimensionless significant wave period of the data in 25 August 1995 to 25 September 1995, is good fit with polynomial degree 4 (the case of least RMSE) of wind speed.

Wave growth with fetch from this data set is given by

$$\begin{aligned} \tilde{H}_s = & -0.07201976\tilde{F}^4 + 0.9725443\tilde{F}^3 - 4.601377\tilde{F}^2 \\ & + 8.861347\tilde{F} + 4.860826 \end{aligned} \quad (4.1.3)$$

Dimensionless wave period with from this data set is given by

$$\begin{aligned} \tilde{T}_s = & -0.03972186\tilde{F}^4 + 0.5214473\tilde{F}^3 - 2.419817\tilde{F}^2 \\ & + 4.660489\tilde{F} - 2.14476 \end{aligned} \quad (4.1.4)$$

For wave growth with duration, we select data that begin at wind speed and wave height are zero or nearly zero as much as, for example shown in Figure 4.1.30. We use multiple linear least-squares fitting with the data set. Wave growth and period with fetch are given by

$$H_s = 0.037(1.64u^{0.23}t^{0.14})^{2.1} \quad (4.1.5)$$

$$T_s = 1.64u^{0.23}t^{0.14} \quad (4.1.6)$$

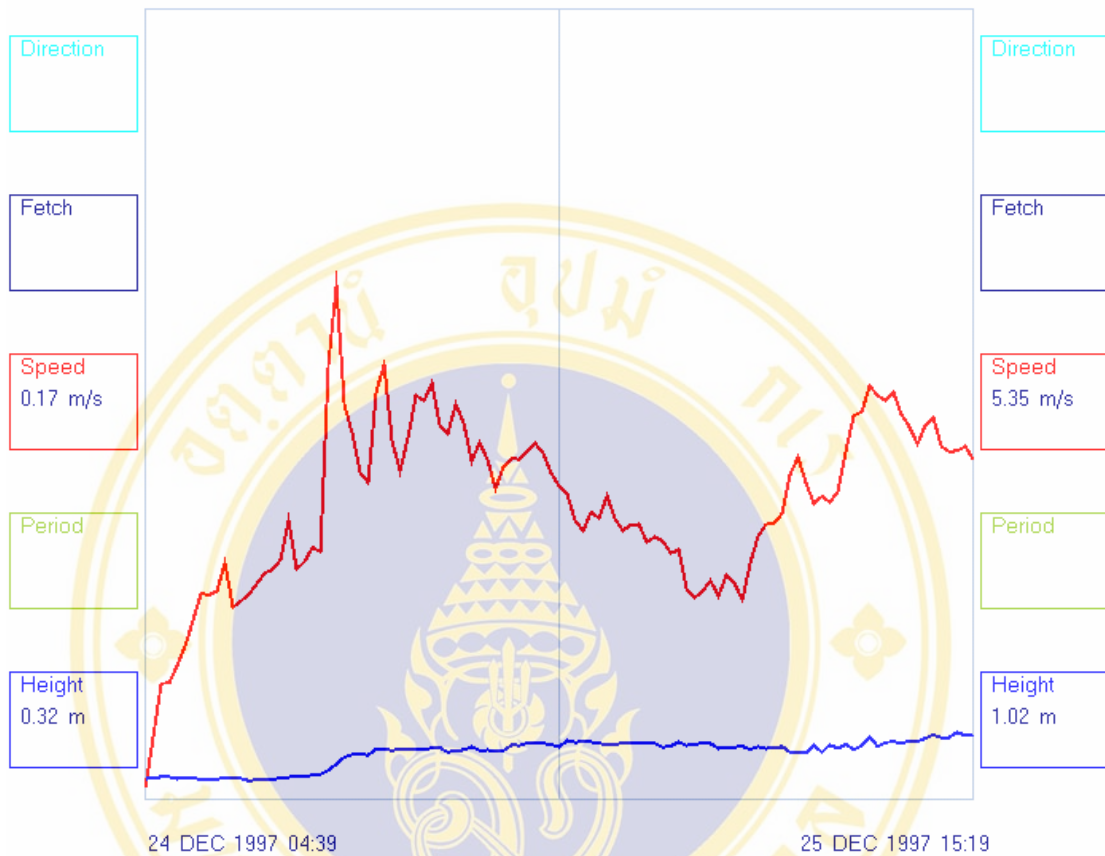


Figure 4.2.29 Shows the begin of data for fitting wave growth with duration

4.3 Results

We adjust the wind speed parameter of the TMA model by using the mean of backward 40 values of the wind speed. We use all of the selected data training the neural network in section 2.4.4 by backpropagation algorithm with $\eta = 0.25$, $\alpha = 0$, and 1000 epochs. We then show scatter plots of observed data and predicted data of the Thompson, SMB, TMA, the developed parametric model, the adjusted parameter of the TMA, and the neural network, shown in Figure 4.3.1 to 4.3.12.

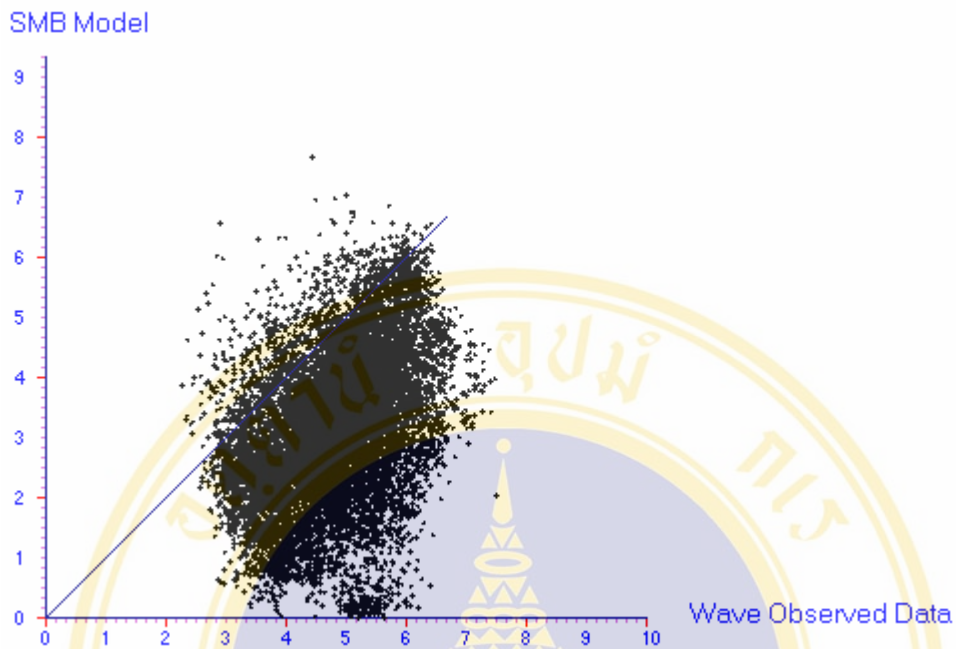


Figure 4.3.1 Scatter plots of the significant wave periods predicted by the SMB model of the all selected data

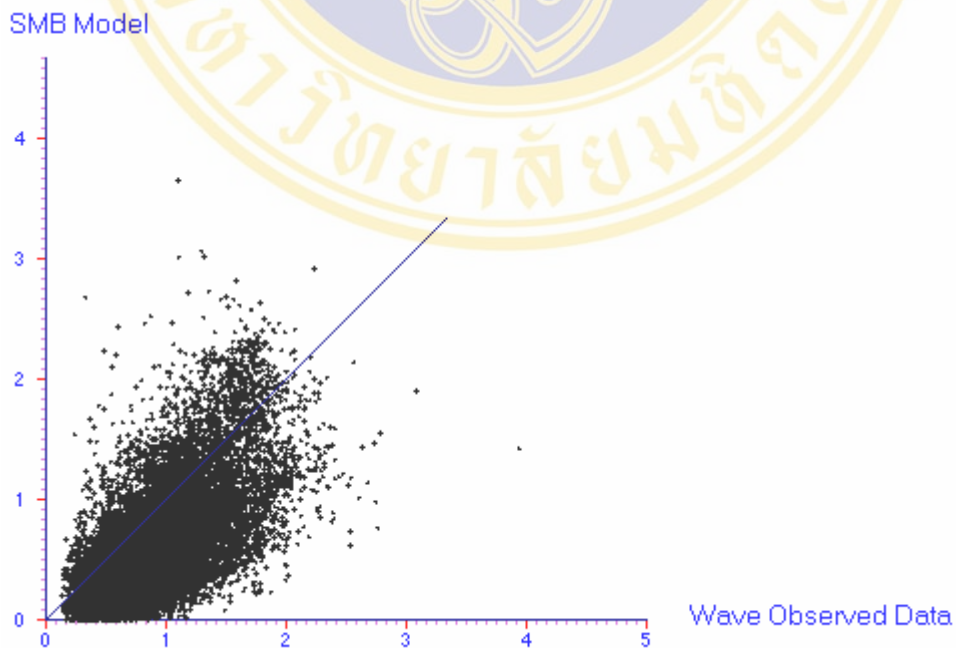


Figure 4.3.2 Scatter plots of the significant wave heights predicted by the SMB model of the all selected data

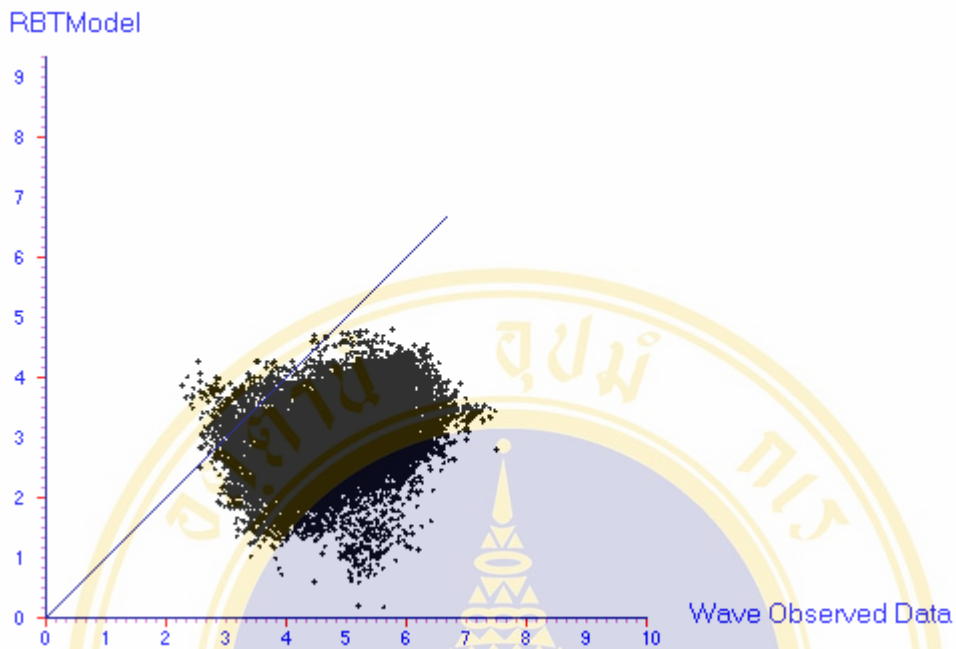


Figure 4.3.3 Scatter plots of the significant wave periods predicted by the Thompson model of the all selected data

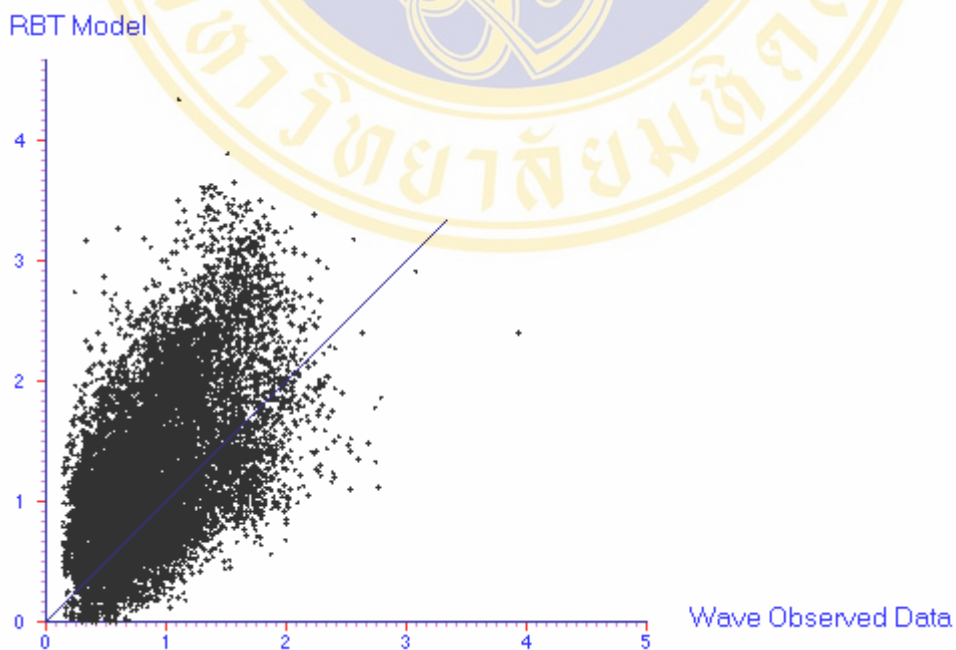


Figure 4.3.4 Scatter plots of the significant wave heights predicted by the Thompson model of the all selected data

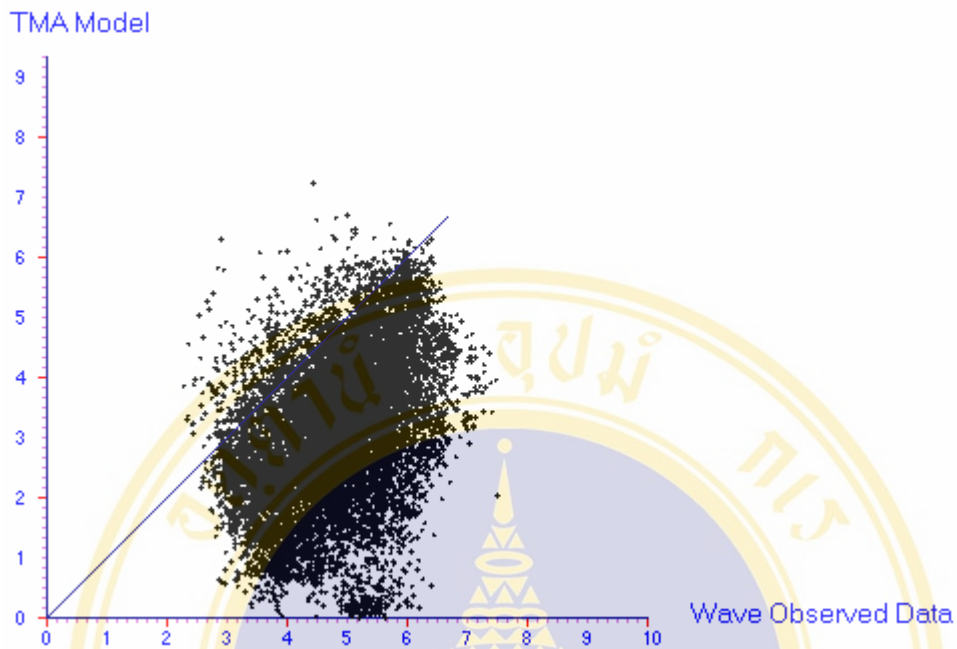


Figure 4.3.5 Scatter plots of the significant wave periods predicted by the TMA model of the all selected data

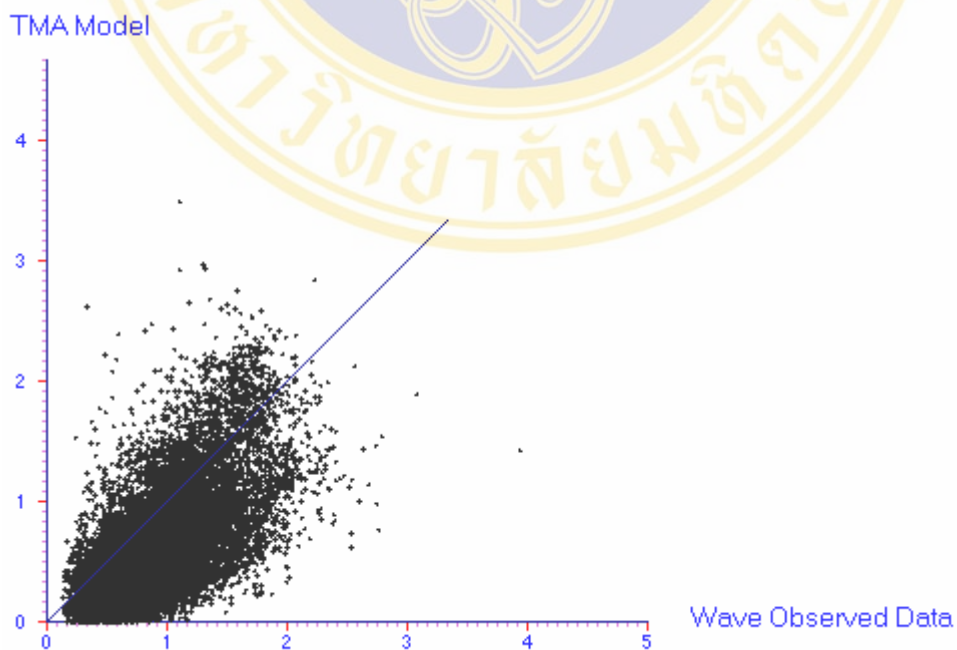


Figure 4.3.6 Scatter plots of the significant wave heights predicted by the TMA model of the all selected data

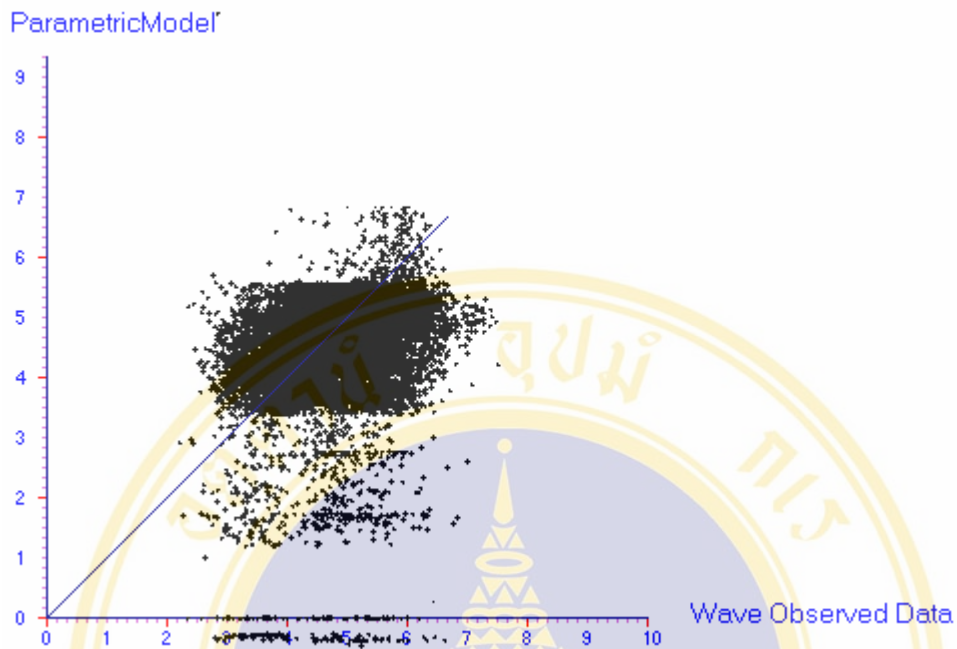


Figure 4.3.7 Scatter plots of the significant wave periods predicted by the developed parametric model of the all selected data

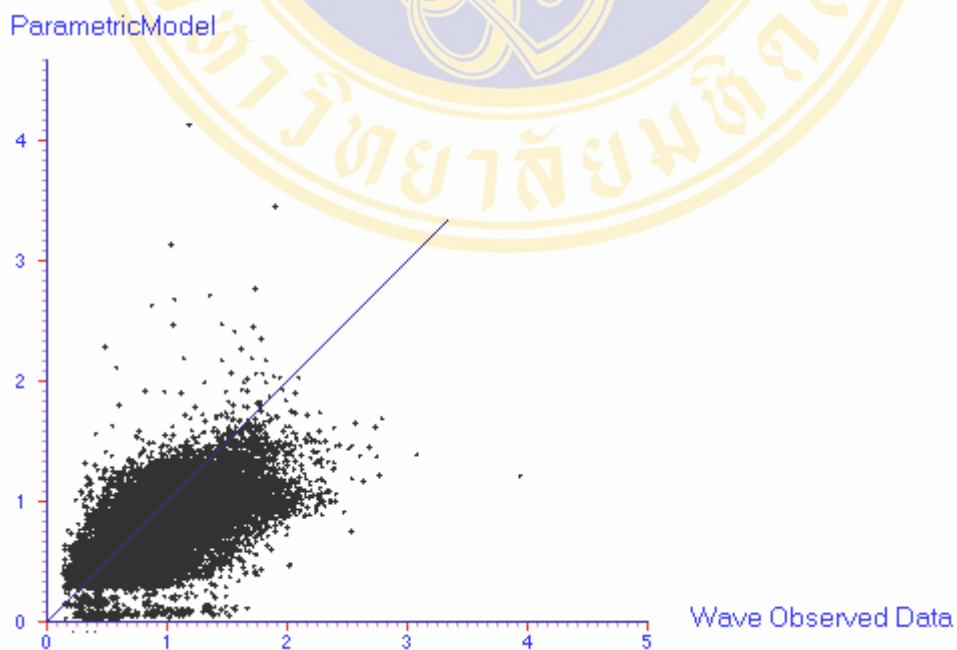


Figure 4.3.8 Scatter plots of the significant wave heights predicted by the developed parametric model of the all selected data

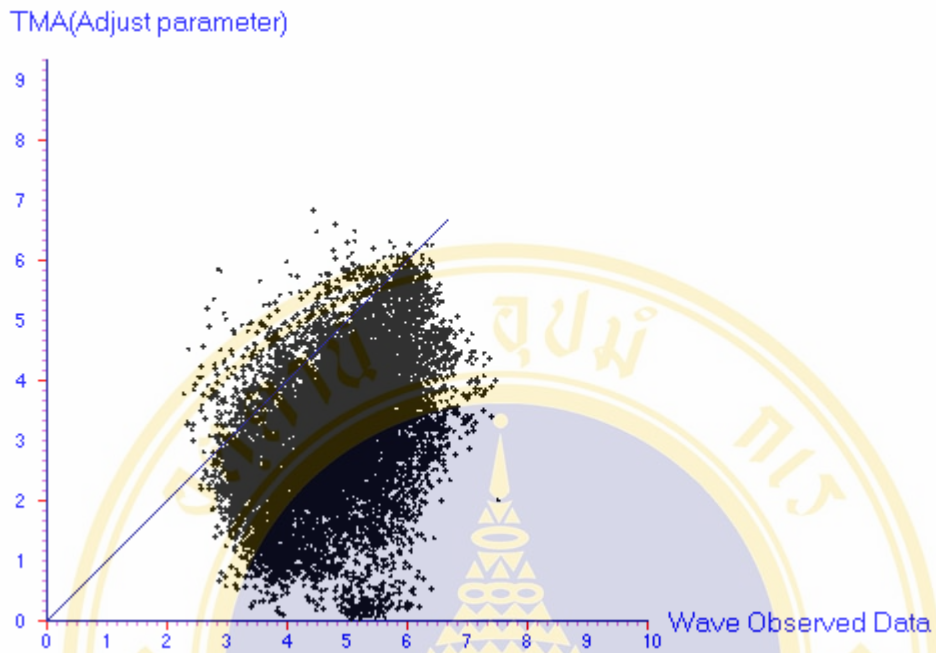


Figure 4.3.9 Scatter plots of the significant wave periods predicted by the adjusted parameter of the TMA of the all selected data

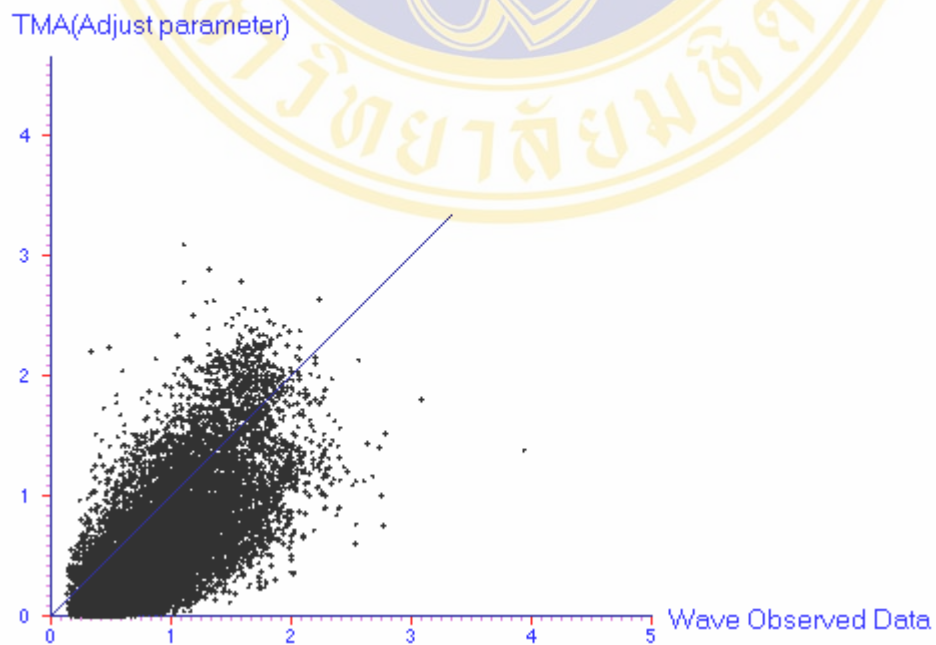


Figure 4.3.10 Scatter plots of the significant wave heights predicted by the adjusted parameter of the TMA of the all selected data

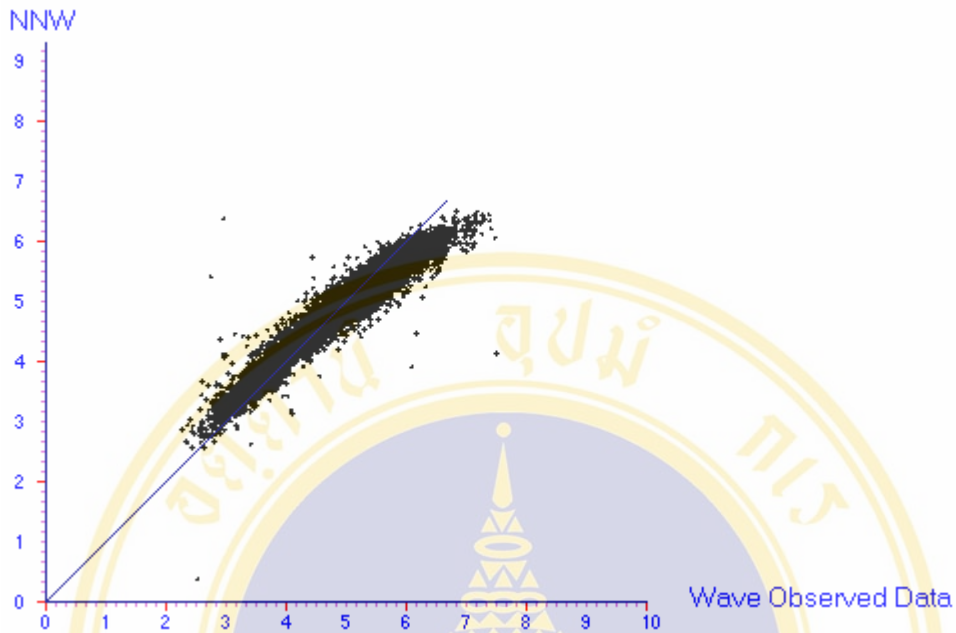


Figure 4.3.11 Scatter plots of the significant wave periods predicted by the trained parametric inputs neural network of the all selected data

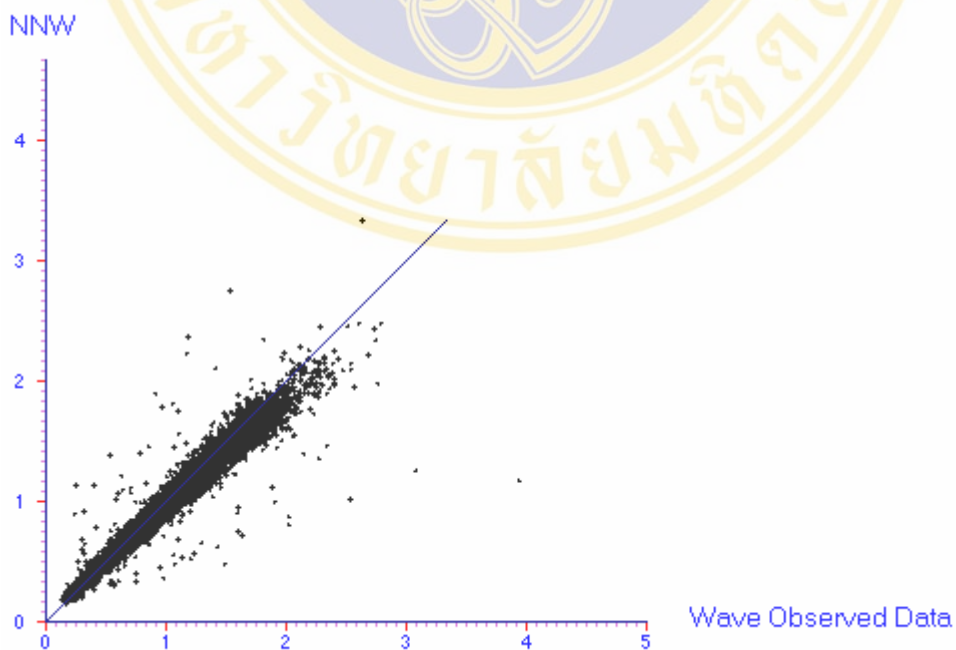


Figure 4.3.12 Scatter plots of the significant wave heights predicted by the trained parametric inputs neural network of the all selected data

We then discuss about the scatter plots in Figure 4.3.1 to 4.3.12. The straight line passes through the plotted points is the line of perfect agreement. If the points are under the line, then the values of the predicted data are smaller than the value of observed data. If the points are over the line, then the values of the predicted data are greater than the value of observed data. Thus we have a good prediction if the points are along the line. However, there are a lot of samples in the data set, it is difficult to compare the performance of prediction results from these figures. Therefore we show the performance of prediction in term of the root mean square error (RMSE) and bias (BIAS) in Table 4.7 and 4.8.

Table 4.7 Root mean square error and bias of the predicted significant wave periods of the all selected data (in year 1995-1998)

Model	SMB	Thompson	TMA	Parametric Model	Adjusted parameter TMA	Neural Net
RMSE	0.425862	0.401883	0.416847	0.376958	0.414610	0.056677
BIAS	-0.336337	-0.364454	-0.314276	-0.073017	-0.340892	0.003002

Table 4.8 Root mean square error and bias of the predicted significant wave heights of the all selected data (in year 1995-1998)

Model	SMB	Thompson	TMA	Parametric Model	Adjusted parameter TMA	Neural Net
RMSE	0.535776	1.06744	0.534920	0.593803	0.522788	0.103960
BIAS	-0.291107	0.558510	-0.291798	-0.145317	-0.294675	-0.004458

It is found from Tables above that arising the parametric models, the adjusted parameter TMA model gives the best results of both the significant wave periods and significant wave heights. However, the use of the neural network model significantly improves the results, which shows the minimum RMSE and BIAS.

CHAPTER V

CONCLUSION

In this research we use data from the UNOCAL buoy station from year 1995-1998 to fit the parametric model. Figure [4.2.2] to figure [4.2.8] show scatter plots of wind directions and speed from year 1995 to 1998. In figure [4.2.2] the mean of wind direction is 124 degrees clockwise from the north, this data nearly represents northeast monsoon. In figure [4.2.3] the mean of wind direction is 256 degrees clockwise from the north, this data nearly represents southwest monsoon. In figure [4.2.4] the mean of wind direction is 255 degrees clockwise from the north, this data nearly represents southwest monsoon. In figure [4.2.5] the mean of wind direction is 134 degrees clockwise from the north, this data represents northeast monsoon. In figure [4.2.6] the mean of wind direction is 252 degrees clockwise from the north, this data represents southwest monsoon. In figure [4.2.7] the mean of wind direction is 90 degrees clockwise from the north, this data nearly represents northeast monsoon.

Then we choose the data in 17 March 1998 to 8 April 1998 to fit the fully developed sea condition. Figure [4.2.9] to figure [4.2.13] show scatter plots least-square fits. It was found that the curve of least-square polynomial degree 5 for significant wave height (for fully developed sea) gives the minimum root mean square error (RMSE). Figure [4.2.14] to figure [4.2.18] display similar results

We choose the data between 25 August 1995 to 25 September 1995 to fit wave growth and wave period with fetch. From figure [4.2.19] to figure [4.2.23] we found that the least-square polynomial degree 4 for significant wave height gives the minimum root mean square error. Figure [4.2.24] to figure [4.2.28] display similar results

We use the mean of backward 40 values of the wind speed and apply with the TMA model. And we try to train the neural network with the parametric inputs of the parametric model. Then we hindcast each models and the results are shown in figure [4.3.1] to figure [4.3.12]. We see that the adjusted TMA has root mean square error

than the TMA model both prediction of significant wave height and significant wave period. We see in the term of root mean square error, shown in table 4.7 and 4.8, that the developed parametric model has minimum of root mean square error of significant wave periods prediction comparing with the others of parametric models. And we see that, shown in table 4.7 and 4.8, the prediction of significant wave heights of the developed parametric model is not much different in the term of root mean square error comparing with the others of parametric models. In all of the results the neural network is best.

In addition, the neural network model was developed and solved by the backpropagation algorithm. The network structures decided by trials and errors. The TMA model was also improved by using the mean past record of wind speed to present the wind speed in the TMA model. It was found from figure[4.3.1] to figure[4.3.12] and Tables 4.7 and 4.8 that among the parametric models, the adjusted parameter TMA model gives the best results of both the significant wave periods and significant wave heights. However, the use of the neural network model significantly improves the results, which shows the minimum RMSE and BIAS.

REFERENCES

1. Albrecht Schmidt. 1996. A Modular Neural Network Architecture with Additional Generalization Abilities for High Dimensional Input Vectors. Master Thesis, Manchester Metropolitan University, UK. Available from: <http://www.teco.uni-karlsruhe.de/~albrecht/neuro/html/report.html> [Accessed 2003 Aug 2].
2. Bouws, E., Gunther, H., and Vincent, C. L. 1985. "Similarity of Wind Wave Spectrum in Finite-Depth Water, Part I: Spectral Form," *J. Geophys. Res.*, Vol 85, No. C3, pp 1524-1530.
3. Bretschneider, C. 1952. "Revised Wave Forecasting Relationships," *Proceedings of the 2nd Coastal Engineering Conference*, American Society of Civil Engineers, pp 1-5.
4. Bretschneider, C. 1990. "Tropical Cyclones," *Handbook of Coastal and Ocean Engineering*, Vol 1, J. B. Herbich, ed., pp 249-270.
5. Donelan, M. A., Hamilton, J., and Hu, W. H. 1982. "Directions Spectra of Wind-Generated Waves," Unpublished manuscript, Canada Centre for Inland Waters.
6. Helmholtz, H. 1888. "Uber Atmospherische Bewwgungen," *S. Ber. Preuss. Akad. Wiss. Berlin, Mathem. Physik Kl.*
7. Jeffreys, H. 1925. "On the Formation of Waves by Wind," *Proc. Roy. Soc. Lond.*, Ser. A., Vol 110, pp 341-347.
8. Kelvin, Lord, 1887. "On the Waves Produced by a Single Impulse in Water of Any Depth or in a Dispersive Medium," *Mathematical and Physical Papers*, Vol IV, London, Cambridge University Press, 1910, pp 303-306.
9. Kitaigorodskii, S. A. 1962. "Application of the Theory of Similarity to the Analysis of Wind Generated Wave Motion as a Stochastic Process," *Bull. Acad. Sci., USSR Ser. Geophys.*, Vol 1, No.1, pp 105-117.

10. Kitaigorodskii, S. A. 1983. "On the Theory of the Equilibrium Range in the Spectrum of Wind-Generated Gravity Waves," *J. Phys. Oceanogr.*, Vol 13, pp 816-827.
11. Miles, J. W. 1957. "On the Generation of Surface Waves by Shear Flows," *Journal of Fluid Mechanics*, Vol3, pp185-204.
12. Myers, Raymond H. 1986. *Classical and Modern Regression with Applications*. Duxbery Press, Boston, Massachusetts, USA.
13. Page, G.F., Gomm J.B. 1993, and Williams D. *Application of Neural Networks to Modelling and Control*. Chapman & Hall, London, UK.
14. Patrick, Lynett. 2001. *Coastal Engineering Manual 2001, Part II-Chapter2*.
15. Phillips, O. M. 1958. "The Equilibrium Range in the Spectrum of Wind-Generated Waves," *Journal of Fluid Mechanics*, Vol 4, pp 426-434.
16. Pierson, W. J., and Moskowitz, L. 1964. "A Proposed Spectral Form for Fully Developed Wind Seas Based in the Similarity Theory of S. A. Kitiagorodskii," *J Geophys. Res.*, Vol 9, pp 5181-5190.
17. Pierson, W. J., Neuman, G., and James, R. W. 1955. "Observing and Forecasting Oceanwaves by Means of Wave Spectra and Statistics," U.S. Navy Hydrographic Office Pub. No. 60.
18. Rumelhart D.E., Hinton G.E. andWilliams R.J., 1986 : *Learning internal representations by error propagation*, in *Parallel Distributed Processing: Explorations in the Microstructures of Cognition*, Vol.I, MIT Press, pp. 318–362
19. Ryan, Thomas P. 1997. *Modern Regression Methods*. New York: Wiley, USA.
20. Snyder, R. L., and Cox, C. S. 1966. "A Field Study of the Wind Generation of Ocean Waves," *J. Mar. Res.*, Vol 24, p 141.
21. Sverdrup, H. U., and Munk, W. H. 1947. "Wind, Sea, and Swell: Theory of Relations for Forecasting." Pub. No. 601, U.S. Navy Hydrographic Office, Washington, DC.
22. Thompson, E. F., and Cardone, V. J. 1996. "Practical Modeling of Hurricane Surface Wind Fields," *Journal of Waterway, Port, Coastal, and Ocean Engineering*, Vol 122, No. 4, pp 195-205.

23. WMO; 1995: Guide to Wave Analysis and Forecasting. Revised edition, draft for final reviews.





APPENDIX

PROGRAM LISTING FOR LEAST SQUARE FITTING

```

private void SqrRgr(float[] coef,float[] xval,float[] yval)
{
    float [,] A = new float[3,3];
    float[] b = new float[3];
    float x,y;

    for(int i =0;i<xval.Length;i++)
    {
        x= xval[i];
        y= yval[i];

        A[0,1] = A[0,1]+x;
        b[0]= b[0]+y;
        b[1]= b[1]+x*y;

        x = x*xval[i];
        A[0,2] = A[0,2]+x;
        b[2]= b[2]+x*y;

        x = x*xval[i];
        A[1,2] = A[1,2]+x;

        x = x*xval[i];
        A[2,2] = A[2,2]+x;

    }

    A[0,0]=xval.Length;

    A[1,0] = A[0,1];

    A[1,1] = A[0,2];
    A[2,0] = A[0,2];

    A[2,1] = A[1,2];

    for(int k=1;k<3;k++)
    {

```

```

x = A[k,0];
for(int i = 0;i<3;i++)
{
    A[k,i] = A[0,0]*A[k,i]/x-A[0,i];
}
b[k] = A[0,0]*b[k]/x-b[0];
}

```

```

x = A[2,1];
A[2,1] = A[1,1]*A[2,1]/x-A[1,1];
A[2,2] = A[1,1]*A[2,2]/x-A[1,2];
b[2] = A[1,1]*b[2]/x-b[1];

coef[2] = b[2]/A[2,2];
coef[1] = (b[1]-coef[2]*A[1,2])/A[1,1];
coef[0] = (b[0]-coef[1]*A[0,1]-coef[2]*A[0,2])/A[0,0];
}

```

```

private void CubeRgr(float[] coef,float[] xval,float[] yval)
{
    float [,] A = new float[4,4];
    float[] b = new float[4];
    float x,y;

    for(int i =0;i<xval.Length;i++)
    {
        x= xval[i];
        y= yval[i];

        A[0,1] = A[0,1]+x;
        b[0]= b[0]+y;
        b[1]= b[1]+x*y;

        x = x*xval[i];
        A[0,2] = A[0,2]+x;
        b[2]= b[2]+x*y;

        x = x*xval[i];
        A[0,3] = A[0,3]+x;
        b[3]= b[3]+x*y;

        x = x*xval[i];
        A[1,3] = A[1,3]+x;

```

```

    x = x*xval[i];
    A[2,3] = A[2,3]+x;

    x = x*xval[i];
    A[3,3] = A[3,3]+x;
}

A[0,0]=wndspd.Length;
A[1,0] = A[0,1];
A[1,1] = A[0,2];
A[2,0] = A[0,2];

A[1,2] = A[0,3];
A[2,1] = A[0,3];
A[3,0] = A[0,3];

A[2,2] = A[1,3];
A[3,1] = A[1,3];

A[3,2] = A[2,3];
for(int k=1;k<4;k++)
{
    x = A[k,0];
    for(int i = 0;i<4;i++)
    {
        A[k,i] = A[0,0]*A[k,i]/x-A[0,i];
    }
    b[k] = A[0,0]*b[k]/x-b[0];
}

for(int k=2;k<4;k++)
{
    x = A[k,1];
    for(int i = 1;i<4;i++)
    {
        A[k,i] = A[1,1]*A[k,i]/x-A[1,i];
    }
    b[k] = A[1,1]*b[k]/x-b[1];
}

x = A[3,2];

```

$$\begin{aligned} A[3,2] &= A[2,2]*A[3,2]/x-A[2,2]; \\ A[3,3] &= A[2,2]*A[3,3]/x-A[2,3]; \\ b[3] &= A[2,2]*b[3]/x-b[2]; \end{aligned}$$

```

coef[3] = b[3]/A[3,3];
coef[2] = (b[2]-coef[3]*A[2,3])/A[2,2];
coef[1] = (b[1]-coef[2]*A[1,2]-coef[3]*A[1,3])/A[1,1];
coef[0] = (b[0]-coef[1]*A[0,1]-coef[2]*A[0,2]-
coef[3]*A[0,3])/A[0,0];
}

```

```
private void Deg4Rgr(float[] coef,float[] xval,float[] yval)
```

```
{
    float [,] A = new float[5,5];
    float[] b = new float[5];
    float x,y;

    for(int i =0;i<xval.Length;i++)
    {
        x= xval[i];
        y= yval[i];

        A[0,1] = A[0,1]+x;
        b[0]= b[0]+y;
        b[1]= b[1]+x*y;

        x = x*xval[i];
        A[0,2] = A[0,2]+x;
        b[2]= b[2]+x*y;

        x = x*xval[i];
        A[0,3] = A[0,3]+x;
        b[3]= b[3]+x*y;
    }
}

```

```

x = x*xval[i];
A[0,4] = A[0,4]+x;
b[4]= b[4]+x*y;

```

```

x = x*xval[i];
A[1,4] = A[1,4]+x;

```

```

x = x*xval[i];
A[2,4] = A[2,4]+x;

```

```
x = x*xval[i];
A[3,4] = A[3,4]+x;
```

```
x = x*xval[i];
A[4,4] = A[4,4]+x;
```

```
}
```

```
A[0,0]=xval.Length;
```

```
A[1,0] = A[0,1];
```

```
A[1,1] = A[0,2];
```

```
A[2,0] = A[0,2];
```

```
A[1,2] = A[0,3];
```

```
A[2,1] = A[0,3];
```

```
A[3,0] = A[0,3];
```

```
A[1,3] = A[0,4];
```

```
A[2,2] = A[0,4];
```

```
A[3,1] = A[0,4];
```

```
A[4,0] = A[0,4];
```

```
A[2,3] = A[1,4];
```

```
A[3,2] = A[1,4];
```

```
A[4,1] = A[1,4];
```

```
A[3,3] = A[2,4];
```

```
A[4,2] = A[2,4];
```

```
A[4,3] = A[3,4];
```

```
for(int k=1;k<5;k++)
```

```
{
```

```
    x = A[k,0];
```

```
    for(int i = 0;i<5;i++)
```

```
    {
```

```
        A[k,i] = A[0,0]*A[k,i]/x-A[0,i];
```

```
    }
```

```
    b[k] = A[0,0]*b[k]/x-b[0];
```

```
}
```

```
for(int k=2;k<5;k++)
```

```
{
```

```

        x = A[k,1];
        for(int i = 1;i<5;i++)
        {
            A[k,i] = A[1,1]*A[k,i]/x-A[1,i];
        }
        b[k] = A[1,1]*b[k]/x-b[1];
    }

    for(int k=3;k<5;k++)
    {
        x = A[k,2];
        for(int i = 2;i<5;i++)
        {
            A[k,i] = A[2,2]*A[k,i]/x-A[2,i];
        }
        b[k] = A[2,2]*b[k]/x-b[2];
    }

    x = A[4,3];
    A[4,3] = A[3,3]*A[4,3]/x-A[3,3];
    A[4,4] = A[3,3]*A[4,4]/x-A[3,4];
    b[4] = A[3,3]*b[4]/x-b[3];

    coef[4] = b[4]/A[4,4];
    coef[3] = (b[3]-coef[4]*A[3,4])/A[3,3];
    coef[2] = (b[2]-coef[3]*A[2,3]-coef[4]*A[2,4])/A[2,2];
    coef[1] = (b[1]-coef[2]*A[1,2]-coef[3]*A[1,3]-
coef[4]*A[1,4])/A[1,1];
    coef[0] = (b[0]-coef[1]*A[0,1]-coef[2]*A[0,2]-coef[3]*A[0,3]-
coef[4]*A[0,4])/A[0,0];
}

```

```

private void Deg4Rgr(float[] coef,float[] xval,float[] yval)
{
    float [,] A = new float[5,5];
    float[] b = new float[5];
    float x,y;

    for(int i =0;i<xval.Length;i++)
    {
        x= xval[i];
        y= yval[i];
    }
}

```

```
A[0,1] = A[0,1]+x;
b[0]= b[0]+y;
b[1]= b[1]+x*y;
```

```
x = x*xval[i];
A[0,2] = A[0,2]+x;
b[2]= b[2]+x*y;
```

```
x = x*xval[i];
A[0,3] = A[0,3]+x;
b[3]= b[3]+x*y;
```

```
x = x*xval[i];
A[0,4] = A[0,4]+x;
b[4]= b[4]+x*y;
```

```
x = x*xval[i];
A[1,4] = A[1,4]+x;
```

```
x = x*xval[i];
A[2,4] = A[2,4]+x;
```

```
x = x*xval[i];
A[3,4] = A[3,4]+x;
```

```
x = x*xval[i];
A[4,4] = A[4,4]+x;
```

```
}
```

```
A[0,0]=xval.Length;
```

```
A[1,0] = A[0,1];
```

```
A[1,1] = A[0,2];
```

```
A[2,0] = A[0,2];
```

```
A[1,2] = A[0,3];
```

```
A[2,1] = A[0,3];
```

```
A[3,0] = A[0,3];
```

```
A[1,3] = A[0,4];
```

```
A[2,2] = A[0,4];
```

```
A[3,1] = A[0,4];
```

```
A[4,0] = A[0,4];
```

$$\begin{aligned} A[2,3] &= A[1,4]; \\ A[3,2] &= A[1,4]; \\ A[4,1] &= A[1,4]; \end{aligned}$$

$$\begin{aligned} A[3,3] &= A[2,4]; \\ A[4,2] &= A[2,4]; \end{aligned}$$

$$A[4,3] = A[3,4];$$

```

for(int k=1;k<5;k++)
{
    x = A[k,0];
    for(int i = 0;i<5;i++)
    {
        A[k,i] = A[0,0]*A[k,i]/x-A[0,i];
    }
    b[k] = A[0,0]*b[k]/x-b[0];
}

for(int k=2;k<5;k++)
{
    x = A[k,1];
    for(int i = 1;i<5;i++)
    {
        A[k,i] = A[1,1]*A[k,i]/x-A[1,i];
    }
    b[k] = A[1,1]*b[k]/x-b[1];
}

for(int k=3;k<5;k++)
{
    x = A[k,2];
    for(int i = 2;i<5;i++)
    {
        A[k,i] = A[2,2]*A[k,i]/x-A[2,i];
    }
    b[k] = A[2,2]*b[k]/x-b[2];
}

```

$$\begin{aligned} x &= A[4,3]; \\ A[4,3] &= A[3,3]*A[4,3]/x-A[3,3]; \\ A[4,4] &= A[3,3]*A[4,4]/x-A[3,4]; \\ b[4] &= A[3,3]*b[4]/x-b[3]; \end{aligned}$$

```

coef[4] = b[4]/A[4,4];
coef[3] = (b[3]-coef[4]*A[3,4])/A[3,3];
coef[2] = (b[2]-coef[3]*A[2,3]-coef[4]*A[2,4])/A[2,2];
coef[1] = (b[1]-coef[2]*A[1,2]-coef[3]*A[1,3]-
coef[4]*A[1,4])/A[1,1];
coef[0] = (b[0]-coef[1]*A[0,1]-coef[2]*A[0,2]-coef[3]*A[0,3]-
coef[4]*A[0,4])/A[0,0];
}

```

```
private void Deg5Rgr(float[] coef,float[] xval,float[] yval)
```

```

{
float [,] A = new float[6,6];
float[] b = new float[6];
float x,y;

for(int i =0;i<xval.Length;i++)
{
x= xval[i];
y= yval[i];

A[0,1] = A[0,1]+x;
b[0]= b[0]+y;
b[1]= b[1]+x*y;

x = x*xval[i];
A[0,2] = A[0,2]+x;
b[2]= b[2]+x*y;

x = x*xval[i];
A[0,3] = A[0,3]+x;
b[3]= b[3]+x*y;

x = x*xval[i];
A[0,4] = A[0,4]+x;
b[4]= b[4]+x*y;

x = x*xval[i];
A[0,5] = A[0,5]+x;
b[5]= b[5]+x*y;

x = x*xval[i];
A[1,5] = A[1,5]+x;
}
}

```

```
x = x*xval[i];
A[2,5] = A[2,5]+x;
```

```
x = x*xval[i];
A[3,5] = A[3,5]+x;
```

```
x = x*xval[i];
A[4,5] = A[4,5]+x;
```

```
x = x*xval[i];
A[5,5] = A[5,5]+x;
```

```
}
```

```
A[0,0]=xval.Length;
```

```
A[1,0] = A[0,1];
```

```
A[1,1] = A[0,2];
```

```
A[2,0] = A[0,2];
```

```
A[1,2] = A[0,3];
```

```
A[2,1] = A[0,3];
```

```
A[3,0] = A[0,3];
```

```
A[1,3] = A[0,4];
```

```
A[2,2] = A[0,4];
```

```
A[3,1] = A[0,4];
```

```
A[4,0] = A[0,4];
```

```
A[1,4] = A[0,5];
```

```
A[2,3] = A[0,5];
```

```
A[3,2] = A[0,5];
```

```
A[4,1] = A[0,5];
```

```
A[5,0] = A[0,5];
```

```
A[2,4] = A[1,5];
```

```
A[3,3] = A[1,5];
```

```
A[4,2] = A[1,5];
```

```
A[5,1] = A[1,5];
```

```
A[3,4] = A[2,5];
```

```
A[4,3] = A[2,5];
```

```
A[5,2] = A[2,5];
```

$$A[4,4] = A[3,5];$$

$$A[5,3] = A[3,5];$$

$$A[5,4] = A[4,5];$$

```

for(int k=1;k<6;k++)
{
    x = A[k,0];
    for(int i = 0;i<6;i++)
    {
        A[k,i] = A[0,0]*A[k,i]/x-A[0,i];
    }
    b[k] = A[0,0]*b[k]/x-b[0];
}

for(int k=2;k<6;k++)
{
    x = A[k,1];
    for(int i = 1;i<6;i++)
    {
        A[k,i] = A[1,1]*A[k,i]/x-A[1,i];
    }
    b[k] = A[1,1]*b[k]/x-b[1];
}

for(int k=3;k<6;k++)
{
    x = A[k,2];
    for(int i = 2;i<6;i++)
    {
        A[k,i] = A[2,2]*A[k,i]/x-A[2,i];
    }
    b[k] = A[2,2]*b[k]/x-b[2];
}

for(int k=4;k<6;k++)
{
    x = A[k,3];
    for(int i = 3;i<6;i++)
    {
        A[k,i] = A[3,3]*A[k,i]/x-A[3,i];
    }
    b[k] = A[3,3]*b[k]/x-b[3];
}

```

```

x = A[5,4];
A[5,4] = A[4,4]*A[5,4]/x-A[4,4];
A[5,5] = A[4,4]*A[5,5]/x-A[4,5];
b[5] = A[4,4]*b[5]/x-b[4];

coef[5] = b[5]/A[5,5];
coef[4] = (b[4]-coef[5]*A[4,5])/A[4,4];
coef[3] = (b[3]-coef[4]*A[3,4]-coef[5]*A[3,5])/A[3,3];
coef[2] = (b[2]-coef[3]*A[2,3]-coef[4]*A[2,4]-
coef[5]*A[2,5])/A[2,2];
coef[1] = (b[1]-coef[2]*A[1,2]-coef[3]*A[1,3]-coef[4]*A[1,4]-
coef[5]*A[1,5])/A[1,1];
coef[0] = (b[0]-coef[1]*A[0,1]-coef[2]*A[0,2]-coef[3]*A[0,3]-
coef[4]*A[0,4]-coef[5]*A[0,5])/A[0,0];
}

private void FitHT(float[] coef,float[] xval,float[] yval)
{
    ArrayList arllogH = new ArrayList();
    ArrayList arllogT = new ArrayList();
    float[] logH,logT;
    float sumH,sumT,sumHT,sumHH,n,det,det1;

    for(int i=0;i<swh.Length;i++)
    {
        if(swh[i]==0 || swp[i] ==0) continue;
        arllogH.Add(Math.Log10(xval[i]));
        arllogT.Add(Math.Log10(yval[i]));
    }
    logH = new float[arllogH.Count];
    logT = new float[arllogH.Count];
    for(int i =0;i<arllogH.Count;i++)
    {
        logH[i] = (float)Convert.ToDouble(arllogH[i]);
        logT[i] = (float)Convert.ToDouble(arllogT[i]);
    }

    //arllogH.Clear();
    //arllogT.Clear();
    n=logH.Length;
    sumH=0;
    sumT=0;

```

```

sumHT=0;
sumHH=0;
for(int i =0;i<logH.Length;i++)
{
    sumH = sumH +logH[i];
    sumT = sumT +logT[i];
    sumHT = sumHT + logH[i]*logT[i];
    sumHH = sumHH + logH[i]*logH[i];
}

det = n*sumHH-sumH*sumH;
det1 = sumT*sumHH-sumHT*sumH;
coef[0] = (float)Math.Pow(10,det1/det);
det1 = n*sumHT-sumH*sumT;
coef[1] = det1/det;
}

private void SqrRgr(float[] coef,float[] xval,float[] yval)
{
    float [,] A = new float[3,3];
    float[] b = new float[3];
    float x,y;

    for(int i =0;i<xval.Length;i++)
    {
        x= xval[i];
        y= yval[i];

        A[0,1] = A[0,1]+x;
        b[0]= b[0]+y;
        b[1]= b[1]+x*y;

        x = x*xval[i];
        A[0,2] = A[0,2]+x;
        b[2]= b[2]+x*y;

        x = x*xval[i];
        A[1,2] = A[1,2]+x;

        x = x*xval[i];
        A[2,2] = A[2,2]+x;
    }

    A[0,0]=xval.Length;

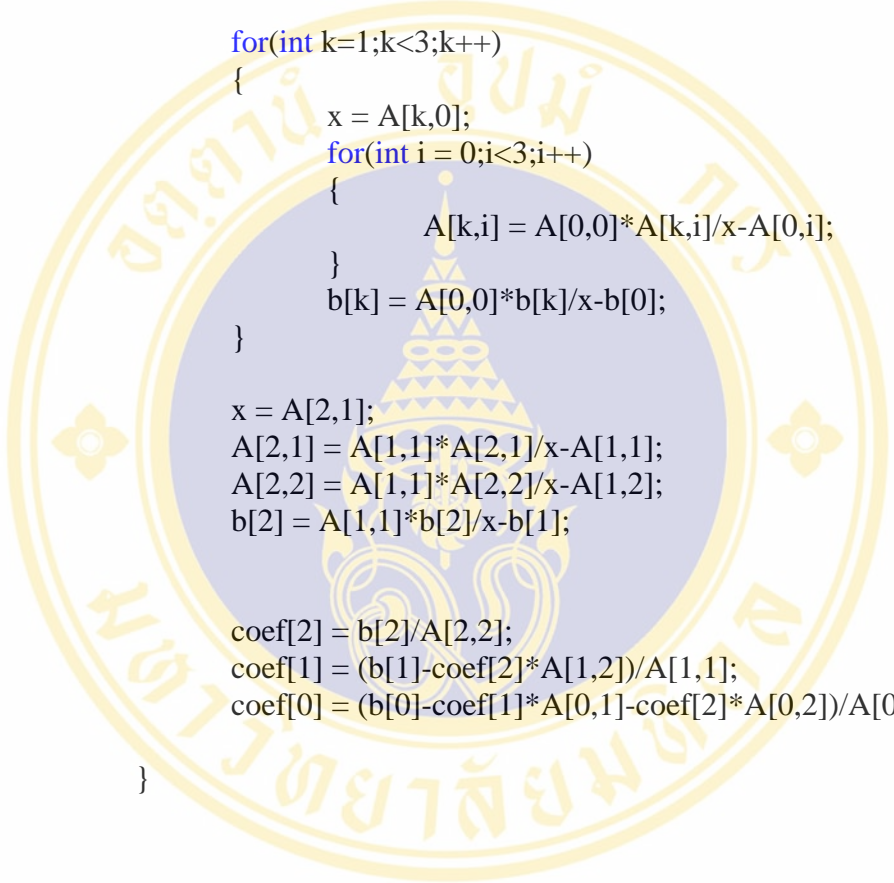
```

$$A[1,0] = A[0,1];$$

$$A[1,1] = A[0,2];$$

$$A[2,0] = A[0,2];$$

$$A[2,1] = A[1,2];$$



```

for(int k=1;k<3;k++)
{
    x = A[k,0];
    for(int i = 0;i<3;i++)
    {
        A[k,i] = A[0,0]*A[k,i]/x-A[0,i];
    }
    b[k] = A[0,0]*b[k]/x-b[0];
}

x = A[2,1];
A[2,1] = A[1,1]*A[2,1]/x-A[1,1];
A[2,2] = A[1,1]*A[2,2]/x-A[1,2];
b[2] = A[1,1]*b[2]/x-b[1];

coef[2] = b[2]/A[2,2];
coef[1] = (b[1]-coef[2]*A[1,2])/A[1,1];
coef[0] = (b[0]-coef[1]*A[0,1]-coef[2]*A[0,2])/A[0,0];
}

```

BIOGRAPHY

NAME	Mr. Charn Khetchaturat
DATE OF BIRTH	3 December 1969
PLACE OF BIRTH	Chaiyaphum, Thailand
INSTITUTIONS ATTENDED	Khonkan University, 1988-1992: Bachelor of Science (Mathematics) Mahidol University, 1998-2003: Master of Science (Applied Mathematics)

